Analysis, Modeling, and Simulation (AMS) Testbed Development and Evaluation to Support Dynamic Mobility Applications (DMA) and Active Transportation and Demand Management (ATDM) Programs

Calibration Report - Chicago

www.its.dot.gov/index.htm
Final Report — October 2016
FHWA-JPO-16-381

U.S. Department of Transportation

Produced by
Booz Allen Hamilton
U.S. Department of Transportation
Intelligent Transportation System (ITS) Joint Program Office (JPO)

Notice

Technical Report Documentation Page

1. Report No. FHWA-JPO-16-381	2. Government Accession No.	3. Recipient's Catalog No.
4. Title and Subtitle Analysis, Modeling, and Simulation (AMS) Testbed Development and Evaluation to Support Dynamic Mobility Applications (DMA) and Active Transportation and Demand Management (ATDM) Programs — Chicago Calibration Report		**5. Report Date** October 2016 **6. Performing Organization Code**
7. Author(s) Balaji Yelchuru, Hani Mahmassani, Ismail Zohdy, Raj Kamalanathsharma		**8. Performing Organization Report No.**
9. Performing Organization Name And Address Booz Allen Hamilton, 20 M Street SE, Suite 1000 Washington, DC - 20003 Subcontractor: Northwestern University		**10. Work Unit No. (TRAIS)** **11. Contract or Grant No.** DTFH61-12-D-00041
12. Sponsoring Agency Name and Address U.S. Department of Transportation Intelligent Transportation Systems–Joint Program Office (ITS JPO) 1200 New Jersey Avenue, SE Washington, DC 20590		**13. Type of Report and Period Covered** **14. Sponsoring Agency Code**

15. Supplementary Notes

FHWA Government Task Manager: James Colyar, Roemer Alfelor

16. Abstract

The primary objective of this project is to develop multiple simulation Testbeds/transportation models to evaluate the impacts of DMA connected vehicle applications and the active and dynamic transportation management (ATDM) strategies. The outputs (modeling results) from this project will help USDOT prioritize their investment decisions for DMA and ATDM programs. One of the unique focus of the Chicago testbed is on Road Weather Connected Vehicle Applications. The Active Traffic Management (ATM) strategies that will be assessed are Dynamic Shoulder Lanes, Dynamic Lane Use Control, Dynamic Speed Limits, and Adaptive Traffic Signal Control. The Active Demand Management (ADM) strategies that will be assessed are Predictive Traveler Information and Dynamic Routing. The Weather-related strategies that will be assessed are snow Emergency Parking Management, Traffic Signal Preemption for Winter Maintenance Vehicles, Snowplow Routing, and Anti-icing and Deicing Operations. From the INFLO Bundle, speed Harmonization (SPD-HARM) will be assessed.

The primary purpose of this report is to document the Calibration process for AMS Chicago Testbed. The report expands on detailed testbed description including the geographic location, modes, operational conditions and cluster analysis details. The report discusses the field observed data used to calibrate the simulation models. Listed in this report are also the margin of error for each calibration effort for each baseline model.

17. Key Words	18. Distribution Statement
ATDM, DMA, AMS, Selection criteria, Testbeds, active transportation demand managements, modeling, dynamic mobility application, weather management strategy, Chicago	

19. Security Class if. (of this report)	20. Security Class if. (of this page)	21. No. of Pages 41	22. Price

Acknowledgements

The Booz Allen Hamilton team thanks the U.S.DOT and project team members for their valuable input.

Name	Organization
Alex Skabardonis	Kittelson & Associates
Brandon Nevers	Kittelson & Associates
Chung Tran	Federal Highway Administration (FHWA)
David Roden	AECOM
James Colyar	Federal Highway Administration (FHWA)
Jim Sturrock	Federal Highway Administration (FHWA)
John Halkias	Federal Highway Administration (FHWA)
Karl Wunderlich	Noblis
Khaled Abdelghany	Southern Methodist University (SMU)
Matthew Juckes	Transport Simulation Systems (TSS)
Meenakshy Vasudevan	Noblis
Peiwei Wang	Noblis
Pitu Mirchandani	Arizona State University (ASU)
Ram Pendyala	Arizona State University (ASU)
Richard Dowling	Kittelson & Associates
Roemer Alfelor	Federal Highway Administration (FHWA)
Sampson Asare	Noblis
Thomas Bauer	Traffic Technology Solutions (TTS)
Xuesong Zhou	Arizona State University (ASU)

Table of Contents

List of Tables

List of Figures

Chapter 1. Introduction

The United States Department of Transportation (USDOT) initiated the Active Transportation and Demand Management (ATDM) and the Dynamic Mobility Applications (DMA) programs to achieve transformative mobility, safety, and environmental benefits through enhanced, performance-driven operational practices in surface transportation systems management. In order to explore a potential transformation in the transportation system's performance, both programs require an Analysis, Modeling, and Simulation (AMS) capability. Capable, reliable AMS Testbeds provide valuable mechanisms to address this shared need by providing a laboratory to refine and integrate research concepts in virtual computer-based simulation environments prior to field deployments.

The foundational work conducted for the DMA and ATDM programs revealed a number of technical risks associated with developing an AMS Testbed which can facilitate detailed evaluation of the DMA and ATDM concepts. Rather than a single Testbed, it is desirable to identify a portfolio of AMS Testbeds in order to (1) capture a wider range of geographic, environmental and operational conditions under which to examine most appropriate ATDM and DMA strategy bundles; (2) add robustness to the analysis results; and (3) mitigate the risks posed by a single Testbed approach. At the conclusion of the initial selection process, five Testbeds were selected to form a diversified portfolio to achieve rigorous DMA bundle and ATDM strategy evaluation: San Mateo (US 101), Pasadena, ICM Dallas, Phoenix and Chicago Testbeds. The analysis plan helps to test the hypotheses of the DMA and ATDM Programs and evaluate the benefits and costs that may be anticipated through their implementation.

The primary purpose of this report is to document the analysis plan approach for the **Chicago** Testbed. The Chicago Testbed is developed for the Chicago core area, which covers around 15 miles from north to south and 10 miles from east to west. A unique feature of the Chicago testbed along the spectrum of conditions exemplified by the five testbeds is the occurrence of sometime severe winter weather, particularly snow episodes which are commonplace for at least four months out of the year. The Testbed area includes the Chicago downtown area, suburbs and cities north of Chicago connecting with major highway sections. These highway sections include the Kennedy Expressway (I-90), the major road connecting downtown Chicago with O'Hare airport, the Edens Expressway (I-94), the major north-south highway connecting downtown Chicago with many of the suburbs and cities north of Chicago, the Dwight D. Eisenhower Expressway (I-290), the major east-west highway connecting downtown Chicago with the western suburbs, and Lakeshore Drive, the mostly freeway-standard expressway running parallel with and alongside the shoreline of Lake Michigan through Chicago.

This Testbed will be used to test several ATDM strategies and DMA bundles considering a proactive network management approach that adopts simulation-based prediction capabilities. Three types of ATDM strategies and one DMA application are proposed for this Testbed. The Active Traffic Management strategies considered consist of: Dynamic Shoulder Lanes, Dynamic Lane Use Control, Dynamic Speed Limits (Basic), Adaptive Traffic Signal Control, Active Demand Management Strategies (consisting of Predictive Traveler Information and Dynamic Routing), as well as Weather-related Strategies (consisting of snow Emergency Parking Management, Traffic Signal Preemption for Winter Maintenance Vehicles, Snowplow Routing and Anti-Icing and Deicing Operations). The DMA application to be tested consists of the Speed Harmonization bundle. The Testbed is developed using the enhanced, weather-sensitive DYNASMART (DYnamic Network Assignment-Simulation Model for Advanced Road Telematics) platform, a discrete time mesoscopic simulation-assignment tool developed, extensively tested, and applied for intelligent transportation system applications.

This report is organized into six chapters as follows:

- Chapter 1 – Introduction: This chapter presents the report overview and objectives.
- Chapter 2 – Testbed Description: This chapter presents the regional characteristics of the Testbed (e.g., geographic characteristic) and the proposed operational conditions, and summarizes the clustered scenarios.
- Chapter 3 – Analysis Plan: This chapter summaries the clustered scenarios for the Chicago Testbed and lists the execution plan. The detailed Analysis Plan is contained in the "Chicago Testbed Analysis Plan" document.
- Chapter 4 – Model Calibration Methodology: This chapter presents the methodology used to calibrate the DYNASMART model of the scenarios selected for the Testbed. The methodology describes the process used to adjust the different model parameters.
- Chapter 5 – Calibration Results: This chapter summarizes the model calibration results. It provides a comparison between the operational conditions observed for each scenario and the corresponding model results.
- Chapter 6 – Summary: This chapter summarizes the report and demonstrates the limitations of the model calibration.

Chapter 2. Testbed Description

The Chicago Testbed network includes Chicago downtown area located in the central part of the network, Kennedy Expressway of I-90, Edens Expressway of I-94, Dwight D. Eisenhower Expressway of I-290, and Lakeshore Drive. The Testbed network is bounded on east by Michigan Lake and on west by Cicero Avenue and Harlem Avenue. Roosevelt Road and Lake Avenue are bounding the Testbed network from south and north, respectively. Figure 2-1 depicts the Chicago Testbed network, and Table 2-1 summarizes characteristics of the network.

Figure 2-1: Map of the Chicago Testbed [Source: Northwestern University]

Table 2-1: Network Characteristics of the Chicago Testbed Network

Network	The Chicago Testbed Network		
Description	• 4,805 links ▪ 150 freeways ▪ 47 highways ▪ 247 ramps (59 are metered) ▪ 4,361 arterials	• 1,578 nodes ▪ 545 signalized intersections	• Demand period ▪ 218 zones ▪ 24 hour ▪ 5 minute interval

The Chicago Weather Testbed is conducive to effective multi-climate congestion management approaches. Table 2-2 shows the relevant weather statistics based on weather data obtained from the Surface Weather Observation Stations (ASOS) O'Hare International Airport station in the past 5 years. The data is in 5-minute interval time resolution and preprocessed to exclude invalid or unrecorded data. It reveals that during the winter season, which stretches from late November to March, snow occurs much more than rain and its relative frequency was over 10% within the past 3 years. Northwestern University (NWU) is the primary developer of the Chicago Weather Testbed, and brings the expertise and experience required to enhance and evaluate weather-related strategies.

Table 2-2: Chicago Weather Event Statistics during Winter

	2009	2010	2011	2012	2013
Clear	80.56%	85.56%	85.91%	92.51%	82.09%
Rain	6.47%	3.77%	7.21%	2.91%	6.25%
Snow	12.40%	12.07%	7.93%	5.12%	11.67%

Both the original Chicago metropolitan region network and the Testbed network experience very large traffic demands during peak hours. As presented in the "Chicago Testbed Analysis Plan" document, the congestion observed along the Edens Expressway in the morning peak is experienced with an average speed of about 25 miles per hour, even lower in the afternoon peak. The congestion becomes much worse in snow season, such that average speed could drop to 10 miles per hour in peak hours. Such conditions are commonly encountered on weekdays during winter. Even though drivers are generally used to driving in such conditions, the weather impact on the overall operational performance is still significant, and calls for innovative technology-enabled approaches to improve overall mobility and traffic congestion management.

Several operational management strategies have been developed for the Chicago Testbed as part of previous or ongoing Northwestern University Transportation Center projects. These strategies focus primarily on (a) real-time traffic estimation and prediction system (TrEPS), incorporating field observations and traffic measures, as well as estimating and predicting network states to enable implementation and evaluation of on-line traffic management; (b) traffic flow model and Weather Adjustment Factor (WAF) calibration with multi-weather effects; and (c) implementation of the multi-modal dynamic network simulation of travelers and vehicles given predicted traveler information. Other strategies have also been developed and tested with DYNASMART on other metropolitan networks under analogous operational conditions: weather-related advisory and control measures for integrated real-time weather responsive traffic management (WRTM) with a Traffic Estimation and Prediction System (TrEPS). These strategies are designed to reduce the impacts of inclement weather events, prevent congestion, and extend the applicability to include sensitivity to dynamic network with predictive information provided.

The dynamics of traffic systems are complex, where many situations necessitate strategies that anticipate unfolding conditions instead of adopting a purely reactive approach. Simulation of the traffic network forms the basis of a state prediction capability that fuses historical data with sensor information under different operational conditions, uses a description of how traffic behaves in networks to predict future conditions, and accordingly develops control measures. A decision support system is needed to map the observed operational conditions to the suitable response plans. The simulation-based traffic performance evaluation and prediction system, DYNASMART, is used to quantify the potential benefits associated with deploying a response plan as recommended by the decision support system

Chapter 3. Analysis Plan

3.1 Cluster Analysis Results

A cluster analysis was performed to determine the main operational conditions on the Chicago Testbed. The detailed approach and results of the cluster analysis are presented in the "Chicago Testbed Analysis Plan" document. Based on the cluster analysis conducted for the Chicago Testbed, four main weather-related clusters are determined. Each cluster includes a specific weather condition and its corresponding traffic flow rate in terms of the attributes that describes operational conditions of these days.

Table 3-1 provides a description of the selected clusters representing operational scenarios for the Chicago Testbed. The table includes the base case under clear weather and other weather-affected traffic cases under rain and snow. Since incident data is not available with the needed spatial and temporal coverage for the cluster analysis, Cluster B-7 is suggested as a hypothetical scenario, a weather-incident mixed scenario.

Table 3-1: The Selected Operational Scenarios for the Chicago Testbed

Variables	All	Cluster B-0	Cluster B-3	Cluster B-4	Cluster C-4	Cluster B-6	Cluster B-7 (hypothetical)
Number of Daily Records	321	67	5	3	4	1	-
Records (%)	100%	21%	2%	1%	1%	1%	-
Cluster Description	AM Peak	High Demand	High Demand	Medium Demand	Low Demand	Medium Demand	Medium Demand
	PM Peak	High Demand	High Demand	High Demand	Medium	High Demand	High Demand
	Incident	None	None	None	None	None	AM Peak
	Daily Weather	Clear / No Rain, No Snow	Moderate/Heavy Rain Changing to Moderate Snow	Moderate Snow	Moderate Snow	Moderate and Heavy Snow	Moderate Snow

3.2 Execution Plan

This section summarizes the process shown in Figure 3-1 used to conduct the analysis for the Chicago Testbed. The analysis scenarios for this Testbed will span three phases to demonstrate and evaluate the applications of ATDM strategies:

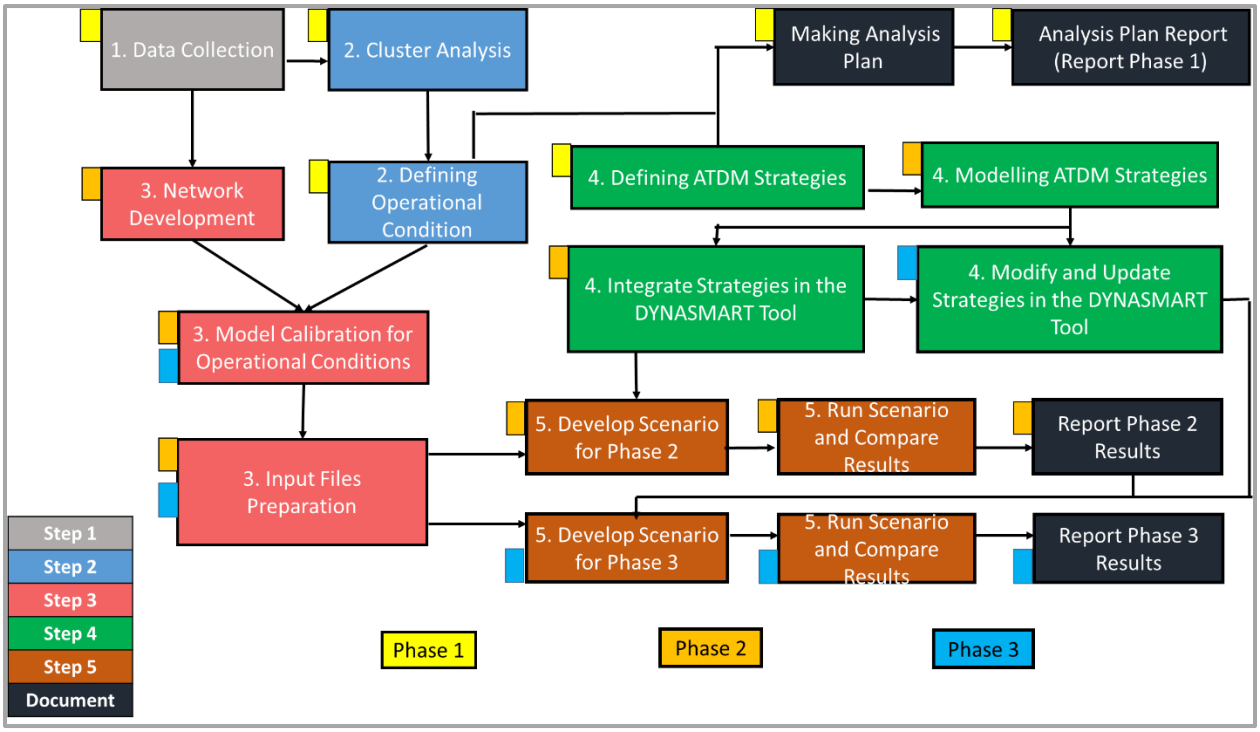

Figure 3-1: Execution Steps and Overview of Project Tasks [Source: NWU]

The team will follow **5 steps** for the **three-Phase** approach to completing the analysis:

Step 1: Data Collection
Step 2: Operational Condition Definition
Step 3: Network Model Calibration
Step 4: Application-Specific Algorithm and Needed Tools
Step 5: Analysis Scenarios

The first two steps have been demonstrated in the Analysis Plan. The following two chapters explain the methodology, progress and the results of network model calibration (Step 3) for the Chicago Testbed.

Chapter 4. Model Calibration Methodology

This chapter describes the methodology used to calibrate the model against the selected scenarios identified through the cluster analysis. This chapter also illustrates how the different model parameters are adjusted such that the observed weather conditions, traffic patterns and associated congestion phenomena are replicated.

4.1 An Overview of the Calibration Methodology

This section provides an overview of the model calibration methodology which can be summarized using the following main steps:

1. Identify the representative daily scenarios for each cluster of operational conditions. A good representative daily scenario should be as close as possible to the core of the cluster (i.e., 5-minute interval averaged traffic flow from the center of the cluster). The detailed representatives of daily scenarios are discussed in the following sections.
2. Obtain the real-world observations for each representative daily scenario. These real-world observations include:
    a. The 5-minute interval precipitation intensity, precipitation type and visibility, which were observed on the selected representative days, from nearby Automated Surface Observing System (ASOS) stations for the Chicago Testbed.
    b. The 5-minute interval traffic volume data, which were observed on the selected representative days, for all freeway detectors in the Chicago Testbed.
    c. The 5-minute interval speed profile, which were observed on the selected representative days, for all freeway detectors in the Chicago Testbed.
3. For the purpose of this study, three model parameter sets are adjusted. These parameters include the parameters of the traffic flow model for the different highway links, the weather adjustment factor (WAF), and the time-dependent OD demand matrix. The parameters of the traffic flow model (i.e., parameters of the modified Greenshield's model that is used to model the vehicle movements on the links) are adjusted such that the model captures the flow and speed patterns along the different highway facilities for different scenarios. The WAF is designed to capture the weather impact on traffic performance in terms of precipitation and visibility. The objective of adjusting the OD demand matrix is to ensure that the model reasonably replicates the observed vehicle counts at the different locations and the associated congestion pattern. The traffic flow models and WAF belong to the supply side parameters, which indicate the capacity and attributes of the traffic network; the time-dependent OD demand matrix is to describe the demand side attributes for the Chicago Testbed.
4. Two sets of calibration procedures are applied to calibrate the model against each scenario day. Following this procedure, the model parameters are adjusted until the model is able to replicate the observed traffic pattern at a satisfactory level. Figure 4-1 graphically displays the calibration procedures, which can be described as:
    a. Supply side parameters: First, the traffic flow model is calibrated under different weather conditions based on pre-defined weather categories (with precipitation type and intensity). The calibrated parameters for the normal weather are supplied to

DYNASMART as the baseline traffic flow model. The parameters under different weather conditions are used to obtain the WAF, which is a reduction factor that reflects the weather impact on each traffic flow parameter. The detailed calibration procedure and the results are discussed in the following sections.

b. Demand side parameters: In order to capture the time-dependent pattern, a bi-level optimization method is used with input files as static/historical OD matrix for the planning time horizon and time-dependent traffic counts on selected observation links. The output is time-dependent OD matrices over the time horizon with a chosen time interval (5 minutes for this project). The normal weather cluster (Cluster B-0) is treated as the base case for selected clusters, and its representative daily scenario is to be calibrated first as the baseline scenario for other representative daily scenarios of other selected clusters (Cluster B-3, B-4, C-4 and B-6). The detailed calibration procedure and the results are discussed in the following sections.

5. Consistency Checking with DYNASMART: The accuracy of the calibration results are verified through the comparison based on acceptable threshold criteria between simulated and field observations. First, the calibrated demand, traffic flow model and WAF are inputs for DYNASMART-P, the simulated link counts are compared with observed link volume. Second, the three inputs are simulated with DYNASMART-X, the estimated and predicted speed from simulation results are compared with the historical observed speed on selected links.

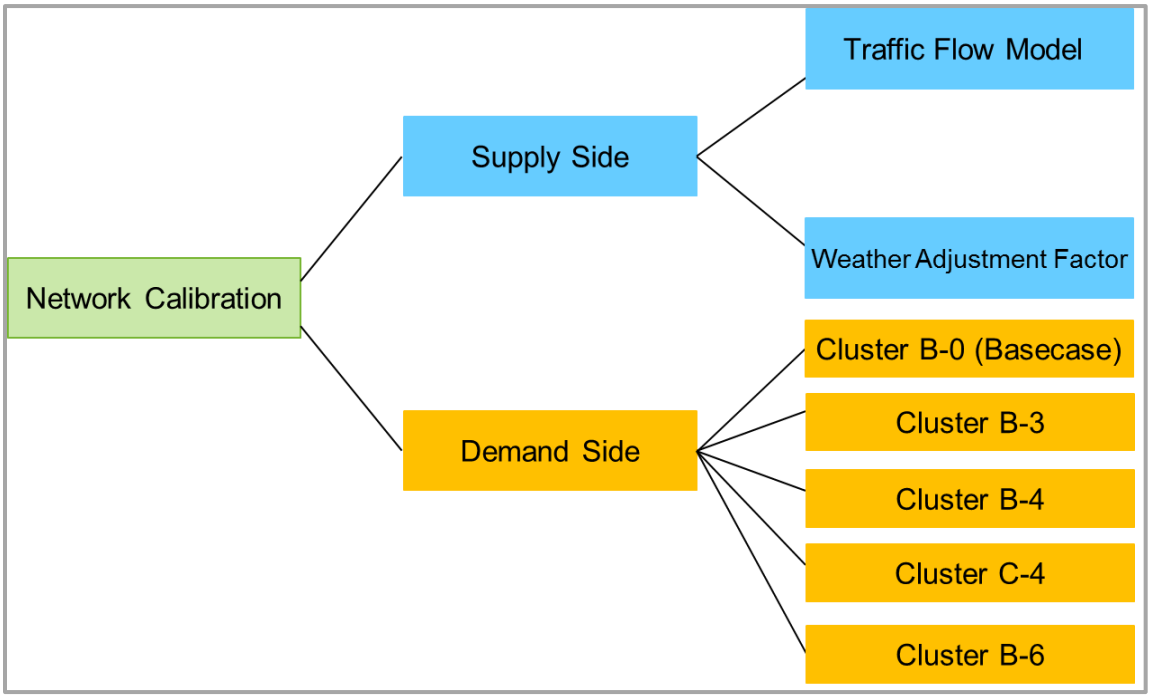

Figure 4-1: Network Calibration Procedures [Source: NWU]

4.2 Supply Side Calibration Methodology

4.2.1 Calibration of Traffic Flow Model Parameters

4.2.1.1 Data Preparation

Traffic data used for the calibration are three major observations from loop detectors, i.e., link volume (or flow rates), occupancy and speed. All traffic data have the aggregation interval of 5 minutes. The occupancy data are further converted into the density using the following relationship[1]:

$$k = \frac{52.8}{L_v + L_s} \cdot occ \tag{4-1}$$

where

k	=	density [veh/mi/lane]
L_v	=	average vehicle length [feet]
L_s	=	average sensor length [feet]
occ	=	occupancy [%]

L_v is assumed to be 5 meters (approximately 16.4 feet); and L_s is set to 2 meters (approximately 6.5 feet) (Mahmassani, Kim et al. 2012). Weather data are collected from nearby Automated Surface Observing System (ASOS) stations located at airports, which contain 5-minute aggregated information of visibility, rain intensity level and snow intensity level. Traffic data and weather data are then matched together according to the timestamps to classify each traffic observation into different weather categories.

4.2.1.2 Modified Greenshields Traffic Flow Model

Two types of modified Greenshields models are used in DYNASMART for traffic propagation. Type 1 is a dual-regime model in which constant free-flow speed is specified for the free-flow conditions (1st regime) and a modified Greenshields model is specified for congested-flow conditions (2nd regime) as shown in Figure 4-2.

[1] Cassidy, M. J. and B. Coifman (1997). "Relation among average speed, flow, and density and analogous relation between density and occupancy." Transportation Research Record: Journal of the Transportation Research Board 1591(1): 1-6.

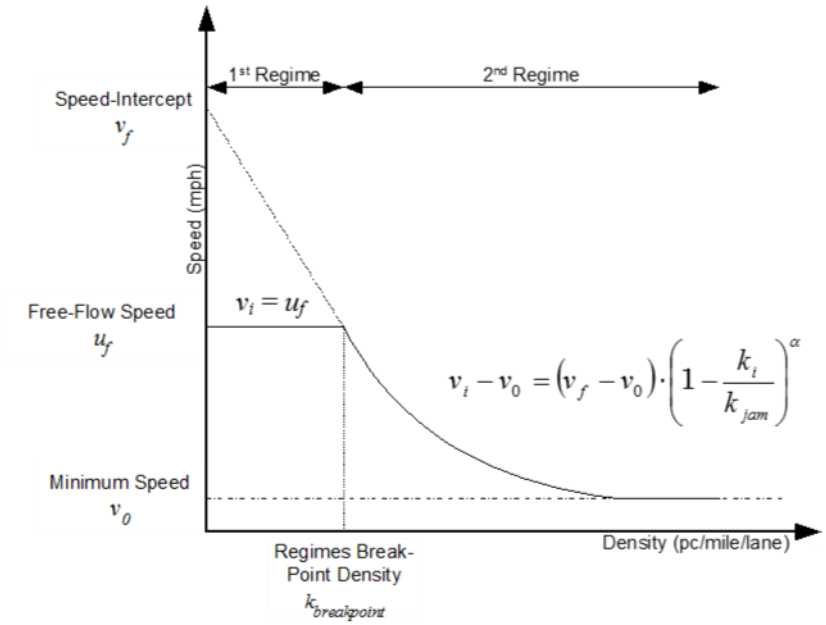

Figure 4-2: Type 1 modified Greenshields model (dual-regime model) [Source: DYNASMART-P User's Guide]

In mathematical terms, the Type 1 modified Greenshields is expressed as follows:

$$v_i = \begin{cases} u_f & 0 < k_i < k_{breakpoint} \\ v_0 + (v_f - v_0)\left(1 - \frac{k_i}{k_{jam}}\right)^{\alpha} & k_{breakpoint} < k_i < k_{jam} \end{cases} \quad (4\text{-}2)$$

where v_i = speed on link *i*

v_f = speed-intercept

u_f = free-flow speed on link *i*

v_0 = minimum speed on link *i*

k_i = density on link *i*

k_{jam} = jam density on link *i*

α = power term

$k_{breakpoint}$ = breakpoint density

Type 2 uses a single-regime to model traffic relations for both free- and congested-flow conditions as shown in Figure 4-3.

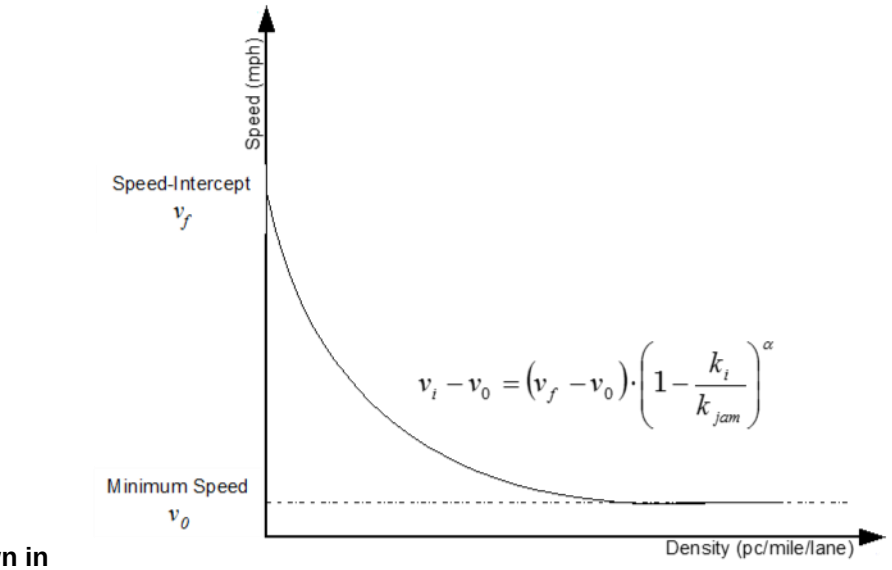

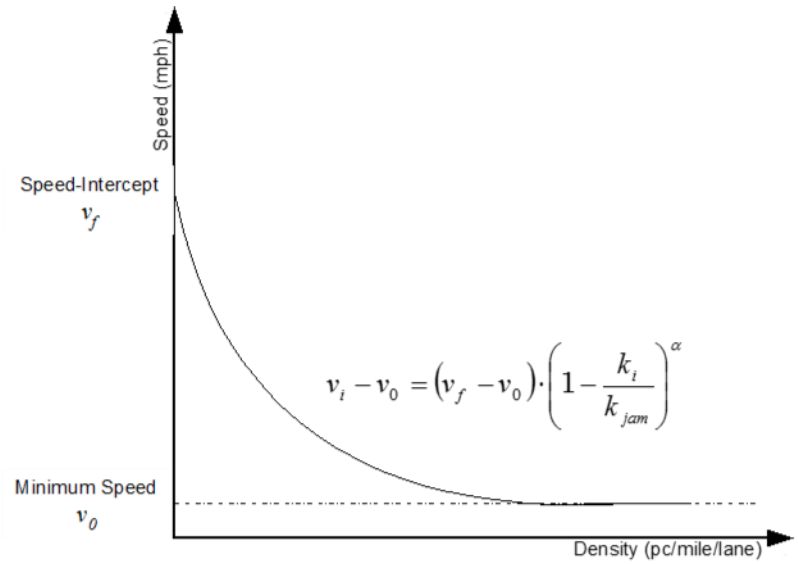

Figure 4-3: Type 2 modified Greenshields model (single-regime model) [Source: DYNASMART-P User's Guide]

In mathematical terms, the type 2 modified Greenshields is expressed as follows:

$$v_i - v_0 = (v_f - v_0) \cdot \left(1 - \frac{k_i}{k_{jam}}\right)^{\alpha} \quad (4\text{-}3)$$

Dual-regime models are generally applicable to freeways, whereas single-regime models apply to arterials. The reason why a two-regime model is applicable for freeways in particular is that freeways have typically more capacity than arterials, and can accommodate dense traffic (up to 2300 pc/hr/ln) at near free-flow speeds. On the other hand, arterials have signalized intersections, meaning that such a phenomenon may be short-lived, if present at all. Hence, a slight increase in traffic would elicit more deterioration in prevailing speeds than in the case of freeways. Therefore, arterial traffic relations are better explained using a single-regime model. All the traffic data used in this study come from loop detectors installed on highways. Therefore the dual-regime model is chosen to fit the collected historical data. For the dual regime model, all six parameters are calibrated, namely, breakpoint density (k_{bp}), free flow speed (u_f), speed-intercept (v_f), minimum speed (v_0), jam density (k_{jam}), and the shape parameter (α). For the single regime model, only three parameters including speed-intercept (v_f), minimum speed (v_0), and the shape parameter (α) are used; jam density (k_{jam}) is assumed to be the density under the "bumper to bumper" traffic condition for the arterial roads.

4.2.1.3 Calibration Procedure and Results

After traffic data are categorized, parameters in the modified Greenshields model are calibrated for each weather condition using a nonlinear regression approach. The following steps describe the procedures for calibrating the dual-regime model, which is used in most cases when traffic data are collected from freeways.

Step 1. Plot the speed vs. density graph, and set initial values for all the parameters, i.e. breakpoint density (k_{bp}), speed-intercept (v_f), minimum speed (v_0), jam density (k_{jam}), and the shape parameter (α), based on observations.

Step 2. For each observed density (k_i), calculate the predicted speed value ($\hat{v}_i$) using Eq.(4-2) and the parameters initialized in Step 1.

Step 3. Compute the squared difference between observed speed value (v_i) and predicted speed value ($\hat{v}_i$), for each data point, and sum the squared error over the entire data set.

Step 4. Minimize the sum of squared error obtained in Step 3, by changing the values of model parameters.

Unlike the linear regression used in earlier research[2], which divides the data into two parts and estimates the two regimes separately, the nonlinear regression used in this study allows estimating the model as a whole, which gives a smooth joint point at the breakpoint density. Step 4 is implemented by Microsoft Excel Solver which uses the generalized reduced gradient algorithm to find the optimal solution. Based on the observed data, the minimum speed (v_0) and jam density (k_{jam}) turn out to be insensitive to weather conditions.

The goodness-of-fit of the nonlinear regression model can be measured by the root mean square error (RMSE) as shown in Eq. (4-4), where $\hat{v}_i$ is the predicted/modeled value and v_i is the observed value for the i^{th} observation in the sample with the size of N. The smaller the RMSE is, the better the model represents the data.

[2] Mahmassani, H. S., J. Dong, J. Kim, R. B. Chen and B. Park (2009). Incorporating weather impacts in traffic estimation and prediction systems, US Department of Transportation, Research and Innovative Technology Administration.

$$RMSE = \sqrt{\frac{1}{N}\sum_{i=1}^{N}(v_i - \hat{v}_i)^2} \quad (4\text{-}4)$$

Another measurement is the R-squared value, which is computed in the same way as in linear regression models. The expression is shown in Eq. (4-5), where represents the mean of the observed data. The R-squared value is the ratio of the regression sum of squares to the total sum of squares, which explains the proportion of variance accounted for in the dependent variable by the model. The closer R-squared value is to 1, the better the model fits the data.

$$R^2 = 1 - \frac{SSE}{SST} = 1 - \frac{\sum(v_i - \hat{v}_i)^2}{\sum(v_i - \bar{v})^2} \quad (4\text{-}5)$$

4.2.2 Calibration of Weather Adjustment Factor (WAF)

4.2.2.1 Weather Categorization

The weather categories were defined based on the precipitation type and the intensity. With a normal weather as the base case, in which no precipitation is observed, three levels of precipitation intensities (light, moderate and heavy) are used for both rain and snow. There are seven weather categories (indices) and the corresponding precipitation intensity ranges: normal (no precipitation), light rain (intensity less than 0.1 in./hr), moderate rain (0.1 to 0.3 in./hr), heavy rain (greater than 0.3 in./hr), light snow (less than 0.05 in./hr), moderate snow (0.05 to 0.1 in./hr), and heavy snow (greater than 0.1 in./hr). The values for the intensity range are based on the literature [3][4][5]

In DYNASMART, supply-side parameters that are expected to be affected by the weather condition are identified as presented in Table 4-1. The inclement weather impact on each of these parameters is represented by a corresponding weather adjustment factor (WAF) such that

$$f_i^{Weather\ \ Event} = F_i \cdot f_i^{Normal} \quad (4\text{-}6)$$

where $f_i^{Weather\,Event}$ denotes the value of parameter *i* under a certain weather event, f_i^{Normal} denotes the value of parameter *i* under the normal condition and F_i is the WAF for parameter *i*.

Table 4-1: Supply Side Properties related with Weather Impact in DYNASMART

Category	*i*	Parameter Description
Traffic flow model[1]	1	Speed-intercept (mph)[1]
	2	Minimal speed (mph)
	3	Density break point (pcpmpl)[1]
	4	Jam density (pcpmpl)
	5	Shape term alpha

[3] Maze, T. H., M. Agarwal and G. Burchett (2006). "Whether weather matters to traffic demand, traffic safety, and traffic operations and flow." Transportation research record: Journal of the transportation research board 1948(1): 170-176.

[4] Rakha, H., M. Farzaneh, M. Arafeh, R. Hranac, E. Sterzin and D. Krechmer (2007). Empirical studies on traffic flow in inclement weather, Virginia Tech Transportation Institute.

[5] Mahmassani, H. S., J. Dong, J. Kim, R. B. Chen and B. Park (2009). Incorporating weather impacts in traffic estimation and prediction systems, US Department of Transportation, Research and Innovative Technology Administration.

Category	*i*	Parameter Description
Link performance	6 7 8	Maximum service flow rate (pcphpl or vphpl) Saturation flow rate (vphpl) Posted speed limit adjustment margin(mph)
Left-turn capacity	9	g/c ratio
2-way stop sign capacity	10 11 12	Saturation flow rate for left-turn vehicles(vphpl) Saturation flow rate for through vehicles(vphpl) Saturation flow rate for right-turn vehicles(vphpl)
4-way stop sign capacity	13 14 15	Discharge rate for left-turn vehicles(vphpl) Discharge rate for through vehicles(vphpl) Discharge rate for right-turn vehicles(vphpl)
Yield sign capacity	16 17 18	Saturation flow rate for left-turn vehicles(vphpl) Saturation flow rate for through vehicles(vphpl) Saturation flow rate for right-turn vehicles(vphpl)

1) only available in dual-regime model; Source: Mahmassani et al. ,2009

The WAF is assumed to be a linear function of weather conditions, and is expressed in the following form

$$F_i = \beta_{i0} + \beta_{i1} \cdot v + \beta_{i2} \cdot r + \beta_{i3} \cdot s + \beta_{i4} \cdot v \cdot r + \beta_{i5} \cdot v \cdot s \quad (4\text{-}7)$$

where

F_i	weather adjustment factor for parameter *i*,
v	visibility (mile),
r	precipitation intensity of rain (inch/hr),
s	precipitation intensity of snow (inch/hr), and
$\beta_{i0}, \beta_{i1}, \beta_{i2}, \beta_{i3}, \beta_{i4}, \beta_{i5}$	coefficients to be estimated.

Thus, once the speed-density functions for different weather conditions (i.e., normal, light rain, moderate rain, etc.) are obtained for each network, a linear regression analysis is performed to obtain the WAF for each parameter based on observed rain intensities, snow intensities and visibility levels. A detailed description of the calibration procedure is provided below.

4.2.2.2 Calibration Procedure

The calibration of coefficients in Eq. (4-7) includes the following steps.

Step 1. For each weather condition c, calculate the WAF for each parameter i such that, where Base denotes the normal (no precipitation) weather.

Step 2. Assign to corresponding traffic-weather data such that each observation has a structure similar to the following:

{time, traffic data (volume, speed, density), weather data(v, r, s), WAF(F1,⋯,Fi)}.

Step 3. For each parameter i, estimate coefficients by conducting the regression analysis using Eq. (4-7) given as a dependent variable and weather data (v, r, s) for all observations as independent variables.

Note that not all of the parameters listed in Table 4-1 can be calibrated using the observation data. Some parameters could be inferred from other calibrated parameters.

1) Traffic flow model related parameters, that is, speed-intercept (v_f), minimum speed(v_0), density break point(k_{bp}), jam density(k_{jam}), shape term alpha(α) and maximum service flow rate (qmax) can be calibrated from the traffic data. However, as minimum speed and jam density turn out to be insensitive to weather conditions from the calibration results, WAF for those parameters are assumed as 1, which indicates these are not affected by weather conditions. In addition, the shape parameter alpha is also fixed as 1 based on the observations that the both speed-intercept (v_f) and alpha(α) govern the shape of the curve and controlling for one variable results in a more consistent and meaningful pattern on the other allowing a better interpretation.
2) Link characteristics: saturation flow rate, and posted speed limit adjustment could be inferred from the calibrated traffic flow model.
3) Signal control: the adjustments in cycle length, offset, green, amber, maximum green, and minimum green could be inferred from the saturation flow rate.
4) Left turn/stop sign/yield sign capacities could be calibrated using the traffic data, for example, maximum observed flow rate could be used as a surrogate of capacity.

4.3 Demand-side Parameter Calibration

Time-dependent (or dynamic) origin-destination (TDOD) matrices are of crucial importance as an input for dynamic traffic assignment (DTA) models. In order to capture the time-dependent pattern, a bi-level

optimization method is used[6]. Specifically, the upper-level problem is a constrained ordinary least-squares problem, which is to estimate the dynamic OD demand based on given link-flow proportions. The link-flow proportions are in turn generated from the dynamic traffic network loading problem at the lower level, which is solved by a DTA simulation in DYNASMART-P. A mathematical programming platform AMPL is used with the solver KNITRO, well-suited for large-scale non-linear problems[7].The solver KNITRO utilizes an interior point/conjugate graduate algorithm in order to converge to the optimum solution in a time-efficient manner[8].

The following notation is used to represent all the variables in the demand estimation formulation. When it comes to the demand estimation using one-day link observations, the subscript of day m is dropped for simplicity.

h : subscript for the observation intervals, during which the traffic volume is accumulated and reported, $h = 1,...H$.

H : number of observation time intervals in the estimation period.

l : subscript for links with traffic flow measurements, $l = 1,...L$.

L : number of links in the network that have flow measurements.

t : subscript for aggregated departure time intervals, $t = 1,...T$.

T : number of aggregated departure time intervals in the estimation period

i : subscript for origin zone, $i = 1,...I$.

I : number of origin zones in the network

j : subscript for destination zone, $j = 1,...J$.

J : number of destination zones in the network,

m : subscript for days of cluster,

M : number of days of cluster, $m = 1,...M$.

$c_{(l,h),m}$: measured traffic volume on link l, during observation interval h, on day m

C_m : vector of measured flows on the links, consisting of element $c_{(l,h),m}$.

$d_{(t,i,j),m}$: demand volume with destination in zone j, originating their trip at zone i during aggregated departure interval t on day m. $d_{(t,i,j),m}$ are the decision variables of this problem and the outputs of the estimation.

D_m : vector of OD demand flows, consisting of elements $d_{(t,i,j),m}$.

$p_{(l,h),(t,i,j),m}$: link-flow proportions, that is the proportion of demand flow $d_{(t,i,j),m}$ that flows onto link l during observation interval h on day m.

P_m : matrix of link-flow proportions, consisting of element $p_{(l,h),(t,I,j),m}$.

[6] Verbas, İ. Ö., H. S. Mahmassani and K. Zhang (2011). "Time-Dependent Origin-Destination Demand Estimation." Transportation Research Record: Journal of the Transportation Research Board 2263(1): 45-56

[7] Waltz, R. and T. Plantenga (2009). Knitro User's Manual: Version 6.0 Ziena Optimization, Inc.

[8] Nocedal, J. and S. J. Wright (2006). Conjugate gradient methods, Springer.

$\varepsilon_{(l,h),m}$: the combined error terms in estimation of traffic flow on link l during observation interval h on day m.

E_m : vector of combined error terms, consisting of element $\varepsilon_{(l,h),m}$ for link flow.

$g_{(i,j)}$: target demand, which is the total traffic demand during period of interest for each origin-destination pair (i, j).

G : target demand vector, which is a vector of total traffic demand during period of interest, consisting of elements $g_{(i,j)}$.

$\eta_{(i,j),m}$: the combined error terms in estimation of total traffic demand during period of interest from zone i to zone j, on day m.

Π_m : vector of combined error terms, consisting of elements $\eta_{(i,j),m}$ for total traffic demand during period of interst.

A : mapping matrix between time-dependent demand and total demand.

w_h : the time weight of deviation between the simulated and the observed link flows for the observation time interval h,

w_l : the link weight of deviation between the simulated and the observed flow for link l.

w_t *and* w_l could be defaulted to be 1 for all links and time intervals. However, different weights may be placed on particular time periods (e.g. peak period) or links (e.g. near major interchange areas) in order to produce TDOD estimates that provide closer fit to areas of concern.

4.3.1 Model with One-day Observations

Two objectives are considered. The first one is to minimize the deviation between observed link flows and estimated link flows, as shown in Eq.(4-8) or (4-9). The second objective is to minimize the deviation between the target demand and estimated demand. Suppose that the target demand is a historical static demand table for the entire simulation horizon, so the second objective function can be explicitly written as the difference between the static demand and the sum of dynamic demand over the period, as shown in Eq. (4-10) or (4-11).

$$C = P \cdot D + E \tag{4-8}$$

or

$$c_{(l,k)} = \sum_{t,i,j} p_{(l,k),(t,i,j)} d_{(t,i,j)} + \varepsilon_{(l,k)} \tag{4-9}$$

$$G = A \cdot D + \Pi \tag{4-10}$$

or

$$g_{(i,j)} = \sum_{t} d_{(t,i,j)} + \eta_{(i,j)} \tag{4-11}$$

Figure 4-4 illustrates the conceptual relationship between these two criteria used in the optimization process. Since the original static/historical OD matrix typically does not agree well with the actual observed link flows, our goal is to find a new time-dependent matrix whose resulting traffic flows are well matched with the observed traffic flows, but at the same time not deviating too much from the original static/historical matrix, which was used as a seed for the new matrix. The final new time-dependent OD matrix is therefore obtained by minimizing both $RMSE_{Flows}$ and $RMSE_{Demand}$ by:

$$RMSE_{Flows} = \sqrt{\frac{\sum_{l=1}^{L}\sum_{t=1}^{T}[M_{l,t} - O_{l,t}]^2}{LT - 1}} \quad (4\text{-}12)$$

$RMSE_{Flows}$ is the measure of error for the deviation between the simulated and the observed link.

$$RMSE_{Demand} = \sqrt{\frac{\sum_{i=1}^{I}\sum_{j=1}^{J}\left[\left\{\sum_{h=1}^{H} d_{i,j,h}\right\} - \delta_{i,j}\right]^2}{IJH - 1}} \quad (4\text{-}13)$$

$RMSE_{Demand}$ is the measure of error for the deviation between the new time-dependent demand.

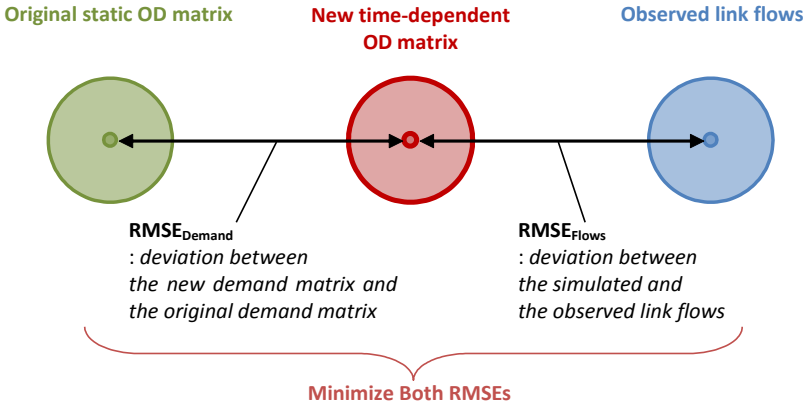

Figure 4-4: Two Criteria in the Optimization Process [Source: NWU]

From a multi-objective programming standpoint, the above bi-objective programming problem can be transformed into a single –objective problem by either a weighting formulation or ε-constraint formulation. The former leads to a relatively simple quadratic programming problem, which coincides with an ordinary linear regression model, while the latter introduces hard non-linear constraints if the deviation is represented by the squared error. The weighted formulation is adopted to combine the two sets of deviations, with respective weights w and (1-w) for the first and second objectives. The weights w and (1-w) could be interpreted as the decision maker's relative preference or importance belief for the different objectives; they could also be considered as the dispersion scales for the first and second error terms in the ordinary least-squares estimation procedure. In general, if the provided target demand is not reliable, i.e. the error term $\eta_{(i,j)}$ has a high variance, a small value of w is used; and vice versa. The resulting bi-level dynamic OD estimation problem with a single day of link-level observations is presented in Eq.(4-14), which is to minimize the combined deviations, subject to the dynamic traffic assignment constraint and non-negativity constraints for demand variables.

$$\min Z = (1-w)(w_h w_l \sum_{l,h} E^2) + w\sum_{i,j} \Pi^2 \quad (4\text{-}14)$$

$$s.t. \quad E = \varepsilon_{(l,h)} = c_{(l,h)} - \sum_{t,i,j} p_{(l,h),(t,i,j)} d_{(t,i,j)}$$

$$\Pi = \eta_{(i,j)} = g_{(i,j)} - \sum_t d_{(t,i,j)}$$

$$p_{(l,h),(t,i,j)} = assignment \left\lfloor d_{(t,i,j)} \right\rfloor \text{ from DTA, } \forall l,h,t,i,j$$

$$d_{(t,i,j)} \geq 0, \forall t,i,j$$

Where w is a positive weight.

If a time-dependent demand matrix is available a priori, $\eta_{(i,j)}$ can be written as Eq. (4-15), where $g_{(i,j)}$ is extended to $g_{(t,i,j)}$ for each departure time interval:

$$\eta_{(i,j)} = \sum_t (g_{(t,i,j)} - d_{(t,i,j)}) \quad (4\text{-}15)$$

The iterative solution algorithm for the proposed bi-level programming problem is briefly described as follows:

Step 1: (Initialization): *ite* = 0. Start from an initial guess of the traffic demand matrix D_0, obtain link-flow proportion P_0 from the DTA simulator.

Step 2: (Optimization): Substituting link-flow proportions P_{ite}, solve the dynamic OD estimation problem as Eq. (4-14) to obtain demand D_{ite}.

Step 3: (Simulation): Using demand D_{ite}, run the DTA simulator to generate new link-flow proportions P_{ite+1}.

Step 4: (Evaluation): Calculate the deviation between simulated link flows and observed link counts, and calculate the deviation between estimated demand D_{ite} and target demand.

Step 5: (Convergence test): The rate of convergence (Eq. (4-16)) is defined as the absolute value of the change of the deviations (including $RMSE_{Flows}$ and $RMSE_{Demand}$) between current iteration and the previous iteration. If the overall rate (Eq. (4-17)) is within 5%, convergence is considered attained for the calibration results. If the convergence criteria are satisfied or if it meets the maximum iterations, *ite*=15, stop the calibration process; otherwise *ite*=*ite*+1 and go to Step 2.

$$R_{ite} = \begin{cases} \dfrac{|RMSE_{ite} - RMSE_{ite-1}|}{RMSE_{ite-1}}, & ite \geq 2 \\ |RMSE_{ite} - RMSE_{ite-1}|, & ite = 1 \end{cases} \quad (4\text{-}16)$$

$$R = R_{ite\_flow} + R_{ite\_demand} \quad (4\text{-}17)$$

How to assess the weight w is the key question for the demand estimation. The weight w is selected through a sensitivity analysis such that the selected weight could give the best trade-off measurement between $RMSE_{Flows}$ and $RMSE_{Demand}$.

4.3.2 Model with Multi-day Observations

The OD demand estimation problem with single-day link observations is extended to a multi-day context. Considering there are n days in one cluster, the Eq. (4-8) and (4-10) can be expressed to more extensive models:

$$\begin{pmatrix} C_1 \\ C_2 \\ \dots \\ C_n \end{pmatrix} = \begin{bmatrix} P_1 & 0 & 0 & 0 \\ 0 & P_2 & 0 & 0 \\ 0 & 0 & \dots & 0 \\ 0 & 0 & 0 & P_n \end{bmatrix} \cdot \begin{pmatrix} D_1 \\ D_2 \\ \dots \\ D_n \end{pmatrix} + \begin{pmatrix} E_1 \\ E_2 \\ \dots \\ E_n \end{pmatrix} \quad (4\text{-}18)$$

$$\begin{pmatrix} G_1 \\ G_2 \\ \dots \\ G_n \end{pmatrix} = \begin{bmatrix} A & 0 & 0 & 0 \\ 0 & A & 0 & 0 \\ 0 & 0 & \dots & 0 \\ 0 & 0 & 0 & A \end{bmatrix} \cdot \begin{pmatrix} D_1 \\ D_2 \\ \dots \\ D_n \end{pmatrix} + \begin{pmatrix} \Pi_1 \\ \Pi_2 \\ \dots \\ \Pi_n \end{pmatrix} \quad (4\text{-}19)$$

Accordingly, E and Π in Eq. (**4-14**) are replaced by the vector $\vec{E} = (E_1, E_2, ...E_n)^T$ and $\vec{\Pi} = (\Pi_1, \Pi_2, ...\Pi_n)^T$.

It is worth mentioning that the individual daily demands in each cluster could be calibrated using the model with multi-day observation; however, in this study, the representative daily scenario for each cluster is of interest.

Chapter 5. Calibration Results

As described above, analyzing the operational conditions in the Chicago testbed has resulted in identifying one base case cluster and four main weather-related clusters that define the dominant operational conditions. A set of representative daily scenarios are identified for each of these clusters as explained in Chapter 2. An intensive calibration effort is then performed to ensure that the model is realistically able to replicate the traffic pattern for each representative scenario. Thus, the model is calibrated to represent five different baseline scenarios.

This chapter summarizes the results of the model calibration effort. It provides a comparison between the model estimation results and the corresponding real-world observations. The results are presented for each representative peak period.

5.1 Representative Daily Scenario Selection

According to clustering analysis, we have five selected existed scenarios and one hypothetical scenario shown in Table 3-1. We select one specific daily scenario from each cluster such that the temporal traffic flow profile for selected scenario is closest to the centroid of the cluster it belongs to. A historical OD demand matrix is given and used as the target demand $g_{(t,i,j)}$ for the detailed OD demand calibration procedure. The selected daily scenarios for each cluster are as follows:

- Cluster B-0: April 22, 2009
- Cluster B-3: February 18, 2009
- Cluster B-4: December 22, 2009
- Cluster C-4: December 19, 2009
- Cluster B-6: January 09, 2009

The selected temporal profiles for weather conditions and traffic demand patterns are shown in Figure 5-1 and Figure 5-2 respectively. The rain/snowprecipitation intensity and the visibility data are from the weather data which is obtained from the ASOS station at O'hare airport.

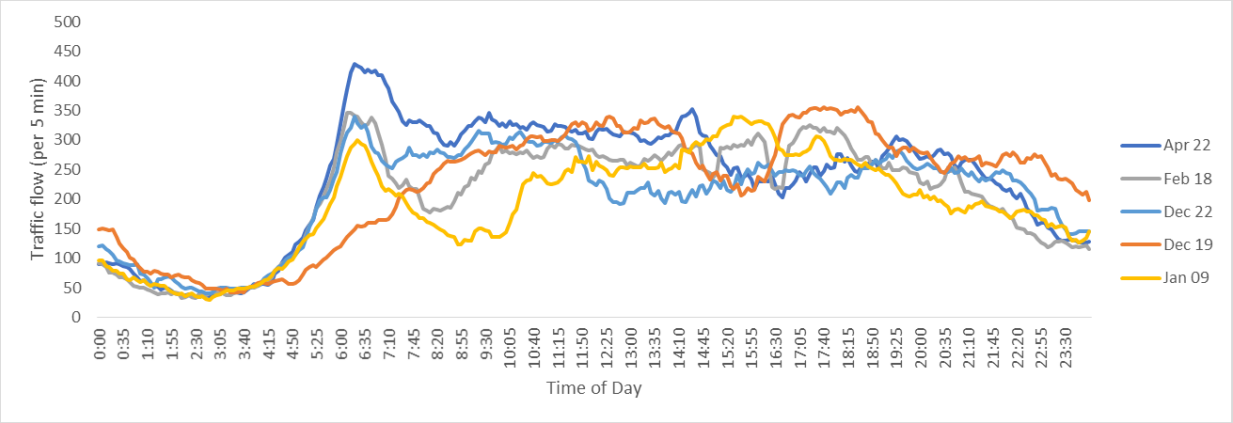

Figure 5-1: Temporal profiles of selected scenarios for traffic flow [Source: NWU]

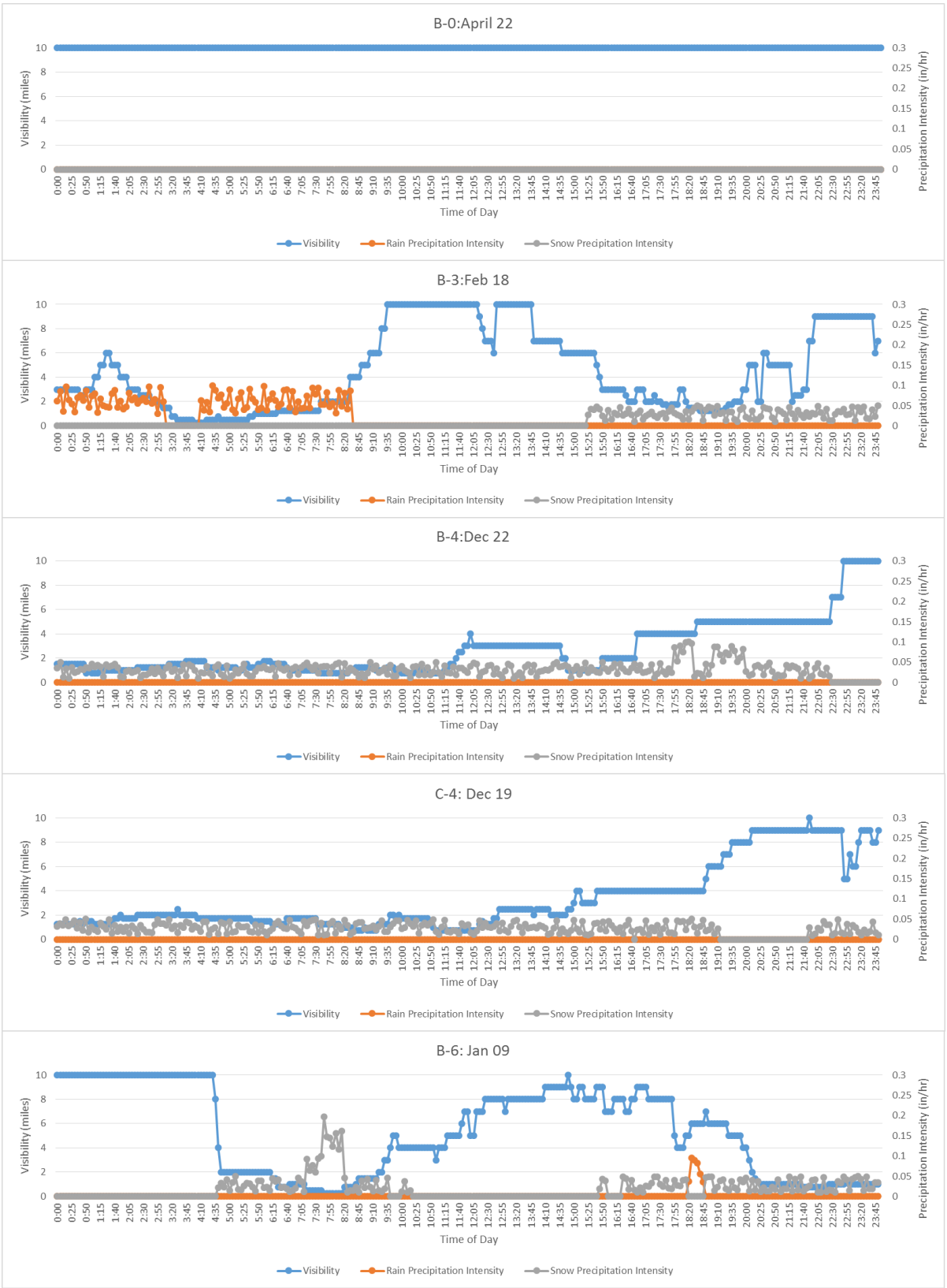

Figure 5-2: Temporal profiles of selected scenarios for weather condition [Source: NWU]

5.2 Traffic Flow Model

The primary source of traffic data is loop detectors installed on freeway lanes. Historical data with the 5-minute interval is obtained from the Illinois DOT in 2009, where the daily 24-hour traffic flow demand profile is described in a vector, which includes 288 5-minute intervals of flow volume.

In the cluster analysis, 13 Illinois DOT loop detectors installed on freeway lanes were selected as a source for the traffic flow and speed data. For the traffic flow model, 9 detectors out of 13 were chosen to provide data for traffic flow model (Figure 5-3). The other four detectors were excluded because their locations were outside the Chicago Testbed network.

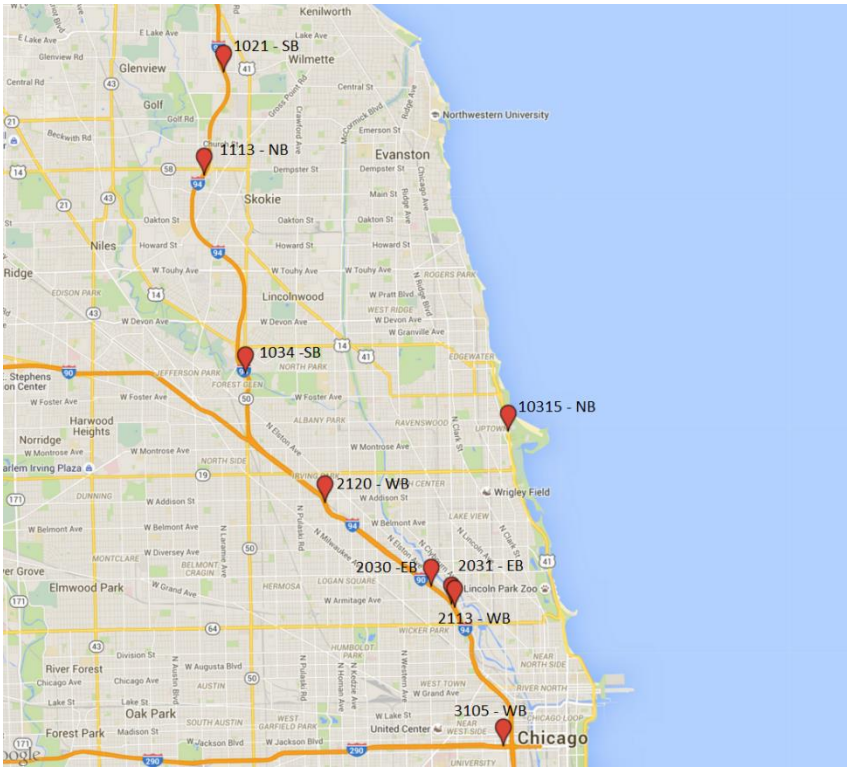

Figure 5-3: Selected Detectors (ID and Directions) for Traffic Flow Model Calibration [Source: Google Maps]

The calibrated speed-density curves for the network are presented in Figure 5-4. It is observed that the overall speed for both uncongested and congested regimes decreases as the weather conditions become severe. The snow event, especially the moderate and heavy snow, causes the clear reductions in speed. Table 5-1 shows the summary of the calibrated parameters based on each detector for the traffic flow model. It is worth mentioning that since the heavy snow condition appeared very rare, and the detectors might be dysfunctional during the adverse weather, some detectors did not provide enough data for traffic flow model calibration of heavy snow weather.

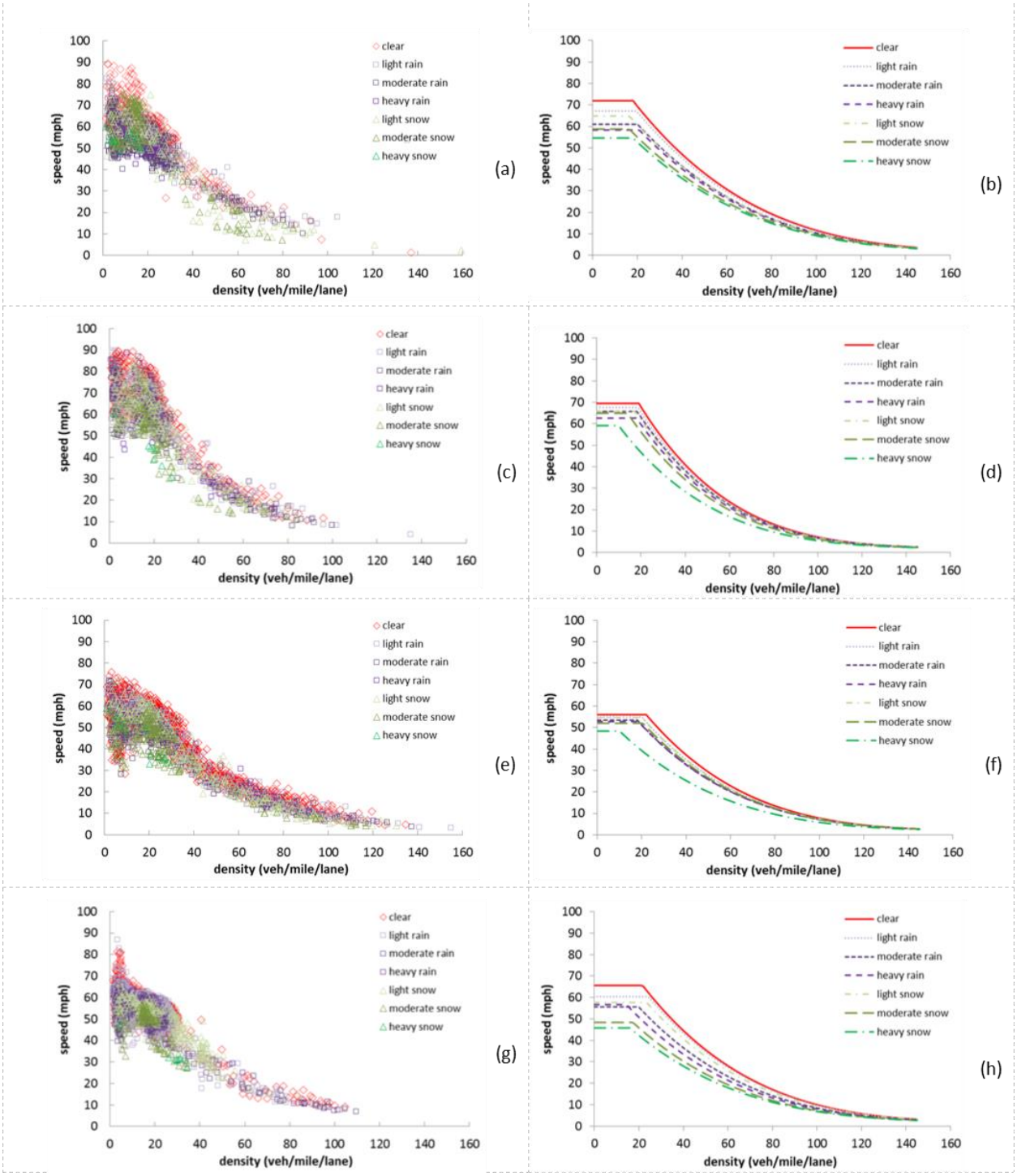
speed (mph)
density (veh/mile/lane)
clear
light rain
moderate rain
heavy rain
light snow
moderate snow
heavy snow
(a)
(b)
(c)
(d)
(e)
(f)
(g)
(h)

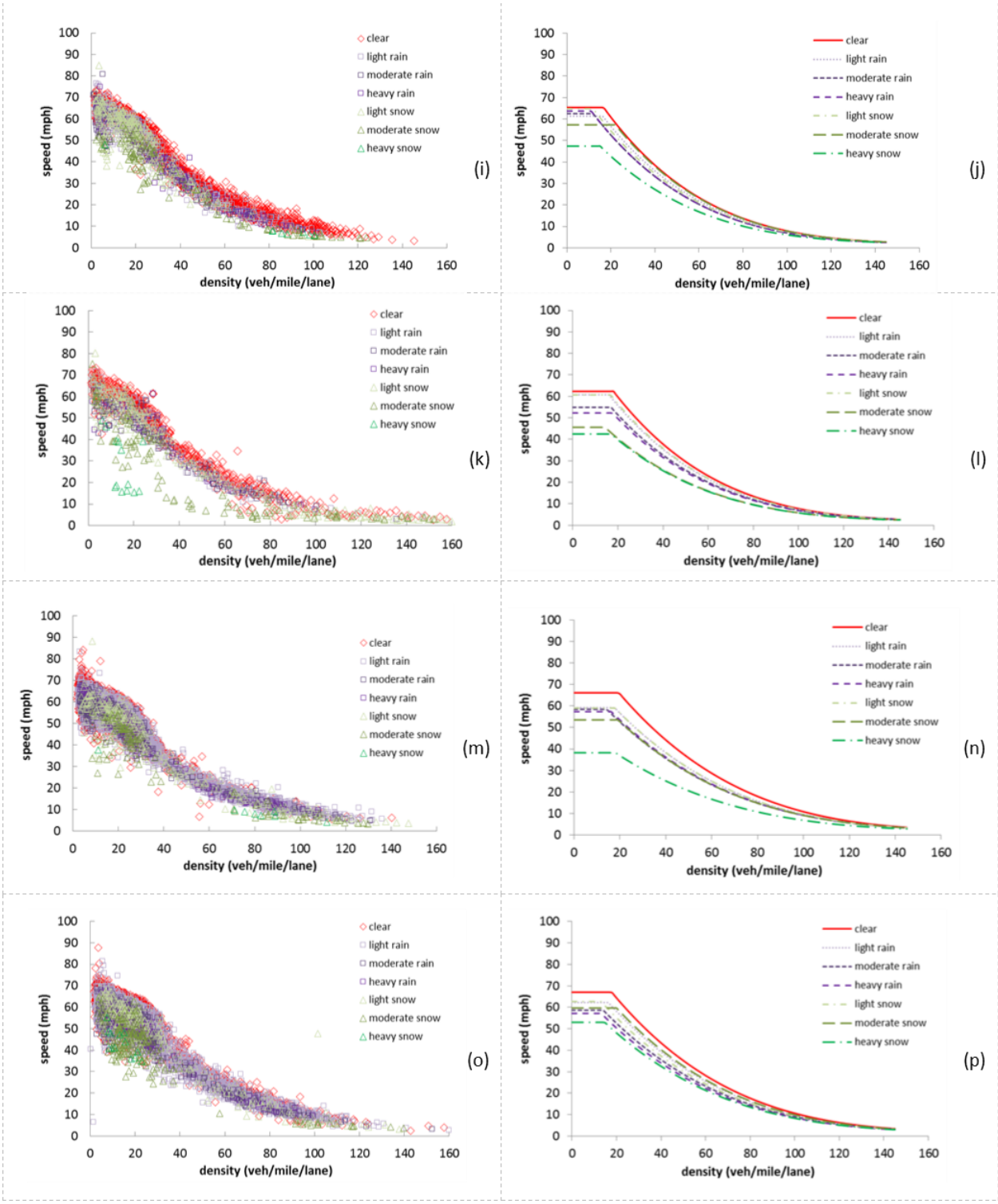
speed (mph)
density (veh/mile/lane)
clear
light rain
moderate rain
heavy rain
light snow
moderate snow
heavy snow
(i)
(j)
(k)
(l)
(m)
(n)
(o)
(p)

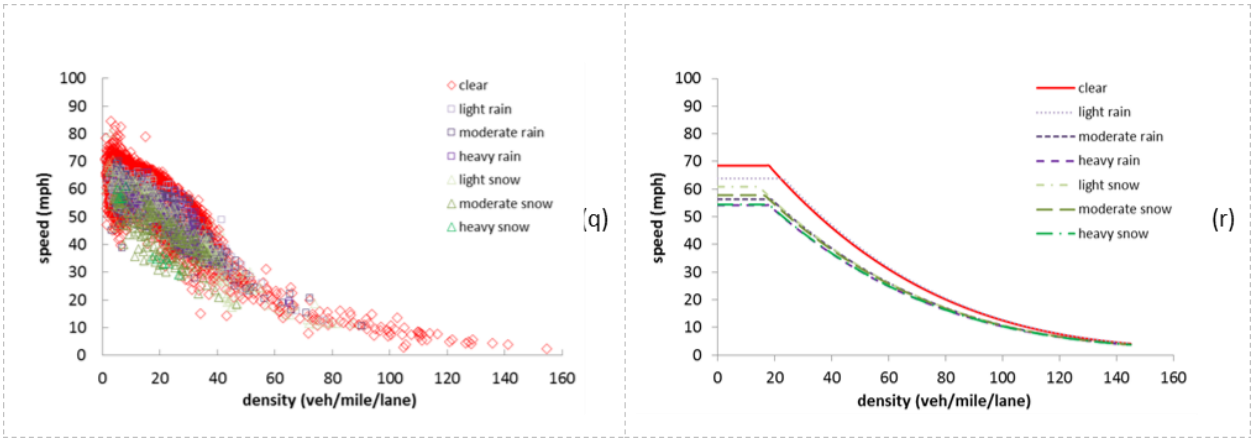

Figure 5-4: Raw traffic data and calibrated speed-density curves under different weather conditions: : (a,b) 1113-NB; (c,d) 1021-SB; (e,f) 1034-SB; (g,h) 3105-WB; (I,j) 2030-EB;(k,l) 2031-EB; (m,n) 2113-WB; (o,p) 2120-WB; (q,r) 10315-NB [Source: NWU]

Table 5-1: Calibrated Parameters for Traffic Flow Model

Highway	Station ID	Weather Condition	qmax (veh/5-min)	v_f (mph)	alpha	k_{bp} (vpmpl)	u_f(mph)	v_0(mph)	k_j (vpmpl)	# of observations		RMSE	R^2
										regime 1	regime 2		
I-94	1113 - NB	normal	567	95.00	3.92	18.00	61.48	2	225	6425	3574	2.68	3.23
		light rain	579	80.19	3.92	19.62	56.80	2	225	4222	3806	8.13	2.96
		moderate rain	504	87.28	3.92	20.10	54.46	2	225	398	336	8.35	5.94
		Heavy Rain	456	89.41	3.92	20.82	54.75	2	225	65	59	7.51	33.58
		light snow	576	86.44	3.92	8.24	84.48	2	225	1327	4020	24.66	7.54
		moderate snow	399	88.41	3.92	16.39	57.02	2	225	135	64	11.20	0.89
		Heavy snow	252	75.00	3.92	18.00	58.25	2	225	13	0	5.37	NA
I-94	1021 - SB	normal	549	108.02	5.12	18.99	75.23	2	225	8256	1743	9.58	0.82
		light rain	522	104.24	5.12	18.67	65.70	2	225	4636	3320	10.71	1.11
		moderate rain	480	100.53	5.12	18.33	65.78	2	225	362	228	11.70	1.20
		Heavy Rain	474	95.11	5.12	18.04	71.18	2	225	50	83	10.09	1.09
		light snow	531	98.12	5.12	17.34	64.42	2	225	3423	1797	10.85	0.81
		moderate snow	369	89.52	5.12	13.98	65.02	2	225	23	87	9.67	1.30
		Heavy snow	264	73.98	5.12	9.92	59.14	2	225	1	7	0.00	0.89
I-94	1034 - SB	normal	576	88.85	4.60	22.06	56.02	2	225	6077	3922	7.07	1.25
		light rain	579	83.38	4.60	20.05	54.98	2	225	3672	4379	7.54	1.22
		moderate rain	570	77.37	4.60	17.95	53.42	2	225	315	408	8.92	1.41
		Heavy Rain	477	77.36	4.60	18.47	52.82	2	225	33	91	6.63	1.24
		light snow	555	82.72	4.60	19.96	54.51	2	225	3086	2473	7.77	1.36
		moderate snow	420	79.52	4.60	20.52	51.93	2	225	92	107	7.46	0.87
		Heavy snow	270	59.40	4.60	5.70	53.01	2	225	2	10	2.10	0.80
I-290	3105 - WB	normal	605	99.93	4.26	21.68	65.60	2	225	4260	5739	3.95	0.49
		light rain	610	97.38	4.26	24.39	60.50	2	225	3373	4602	4.18	0.42
		moderate rain	530	81.74	4.26	16.95	54.10	2	225	261	334	4.49	0.91
		Heavy Rain	510	74.62	4.26	14.51	56.66	2	225	31	102	3.49	0.83
		light snow	609	91.31	4.26	23.55	57.76	2	225	2293	2942	5.06	0.15
		moderate snow	437	67.47	4.26	17.39	62.67	2	225	60	50	4.85	0.79
		Heavy snow	403	62.00	4.26	16.00	50.93	2	225	0	8	NA	0.95
I-90	2030 - EB	normal	764	92.69	4.65	16.67	65.40	2	225	3627	6372	4.82	1.02
		light rain	780	85.85	4.65	16.16	61.29	2	225	2231	5733	5.34	1.01
		moderate rain	736	79.76	4.65	11.82	62.50	2	225	194	401	5.88	1.01
		Heavy Rain	668	79.89	4.65	10.90	63.83	2	225	17	115	5.91	1.04
		light snow	736	82.56	4.65	11.81	64.70	2	225	1647	3583	7.56	0.85
		moderate snow	592	91.22	4.65	24.93	53.68	2	225	13	97	2.72	0.97
		Heavy snow	272	64.50	4.65	15.00	47.35	2	225	0	8	NA	1.09
I-90	2031 - EB	normal	304	91.00	4.66	18.00	62.34	2	225	5448	4551	29.84	3.00
		light rain	780	85.00	4.66	16.08	60.75	2	225	2436	5620	14.20	1.32
		moderate rain	780	78.15	4.66	17.00	54.80	2	225	440	295	15.71	1.52
		Heavy Rain	780	75.75	4.66	17.71	59.16	2	225	86	41	16.64	1.16
		light snow	712	86.38	4.66	16.82	60.75	2	225	2368	3185	20.62	1.09
		moderate snow	560	61.20	4.66	14.35	45.55	2	225	21	177	22.10	1.79
		Heavy snow	420	60.37	4.66	17.00	42.47	2	225	13	0	12.59	NA
I-90	2113 - WB	normal	792	94.37	4.00	19.60	59.21	2	225	3750	6249	4.20	0.74
		light rain	776	81.19	4.00	17.59	59.18	2	225	2817	5144	9.90	1.04
		moderate rain	708	75.33	4.00	10.28	62.82	2	225	161	428	4.28	0.94
		Heavy Rain	652	76.78	4.00	10.18	64.14	2	225	15	117	4.27	1.12
		light snow	728	81.39	4.00	17.87	57.58	2	225	1526	3708	6.19	0.79
		moderate snow	552	75.59	4.00	19.17	53.54	2	225	36	74	8.09	1.12
		Heavy snow	284	52.67	4.00	18.00	34.00	2	225	0	8	NA	1.04
I-90	2120 - WB	normal	788	92.45	3.99	17.85	62.72	2	225	5311	4688	4.42	0.91
		light rain	820	83.48	3.99	16.44	62.19	2	225	3412	4639	4.94	0.99
		moderate rain	744	75.57	3.99	14.12	58.80	2	225	270	464	4.92	0.93
		Heavy Rain	680	72.21	3.99	13.20	57.17	2	225	26	101	6.08	0.85
		light snow	832	79.35	3.99	13.15	69.90	2	225	1928	3631	6.23	0.72
		moderate snow	576	85.81	3.99	20.13	59.66	2	225	116	83	7.72	1.80
		Heavy snow	352	68.93	3.99	14.78	60.66	2	225	7	6	4.93	0.79
Lake Shore	10315 - NB	normal	552	92.18	3.65	18.00	62.62	2	225	1614	8385	0.43	0.32
		light rain	546	94.17	3.65	23.18	66.00	2	225	4199	3235	21.47	0.58
		moderate rain	507	76.73	3.65	19.86	49.63	2	225	465	147	25.63	0.86
		Heavy Rain	495	72.85	3.65	18.00	63.11	2	225	87	11	25.86	1.19
		light snow	534	76.96	3.65	14.52	60.76	2	225	3830	471	27.08	2.13
		moderate snow	405	75.82	3.65	16.49	52.61	2	225	151	23	18.78	0.35
		Heavy snow	228	73.19	3.65	18.00	58.94	2	225	4	8	1.49	0.99

5.3 Weather Adjustment Factor

Based on the calibrated traffic model of the four highways, i.e. I-90, I-94, I-290 and LakeShore Drive, it is found that the maximum service flow rate (q_{max}), shape parameter (α), and free flow speed (u_f), are sensitive to both rain and snow intensities. As the rain or snow intensity increases, maximum flow rate, speed intercept and free flow speed are reduced. The effects of the rain intensity and the snow intensity on different traffic flow model parameters are presented in Figure 5-5.

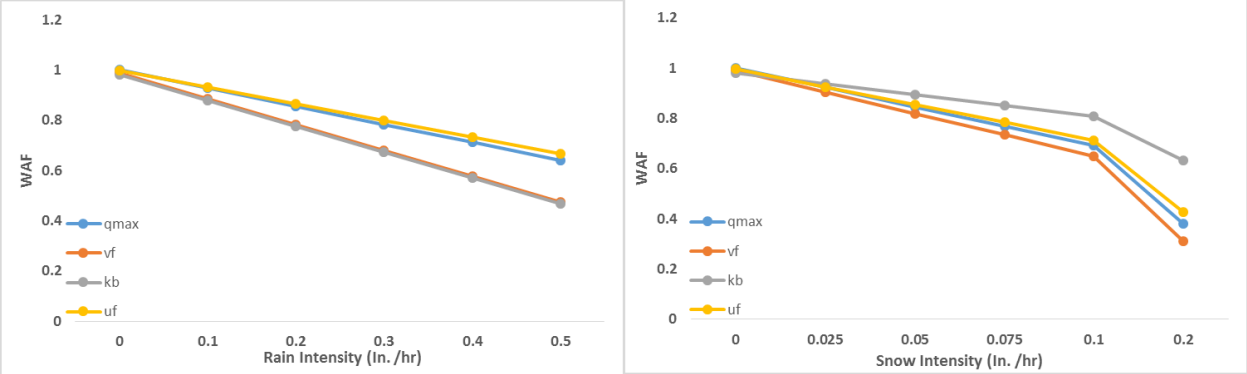

Figure 5-5: Effect of the rain and snow intensity on weather adjustment factors [Source: NWU]

The calibration results of WAF for the three networks are provided in Table 5-2. The low R-squared values of breakpoint density (k_{bp}) suggest that this parameter is insensitive to visibility and precipitation intensity levels.

Table 5-2: Calibration results of WAF

Network	Parameter	β_0	β_1	β_2	β_3	β_4	β_5	R^2
Chicago	q_{max}	0.9979	0.0003	-0.3312	-3.0583	-0.0436	-0.0046	0.6919
	v_f	0.9254	0.0071	-0.1071	-1.6901	-0.1026	-0.1902	0.9061
	k_b	0.8713	0.0122	0.5052	0.1758	-0.1700	-0.2138	0.2413
	u_f	0.9702	0.0029	-0.2695	-1.8068	-0.0437	-0.1150	0.7569

5.4 Time-Dependent OD Matrix

This section discusses the estimation results for the time-dependent OD matrix for all selected scenarios. For each scenario, we present the convergence pattern of the optimization process for obtaining the final OD matrix and the resulting time-dependent demand profile.

5.4.1 Data Source

The required inputs to the OD estimation framework are: (a) static or historical OD matrix for the planning time horizon; and (b) time-dependent traffic counts on selected observation links.

The data source we used to construct the historical demand profile was a 5-minute interval, 5-hr (5am – 10am) demand obtained from Implementation and Evaluation of Weather Responsive Traffic Estimation and Prediction System Project (TrEPS). We then extended the 5-hr demand to 24-hr demand (Figure 5-6) for the Chicago Testbed, by applying multiplication factors to other time periods based on link counts observations.

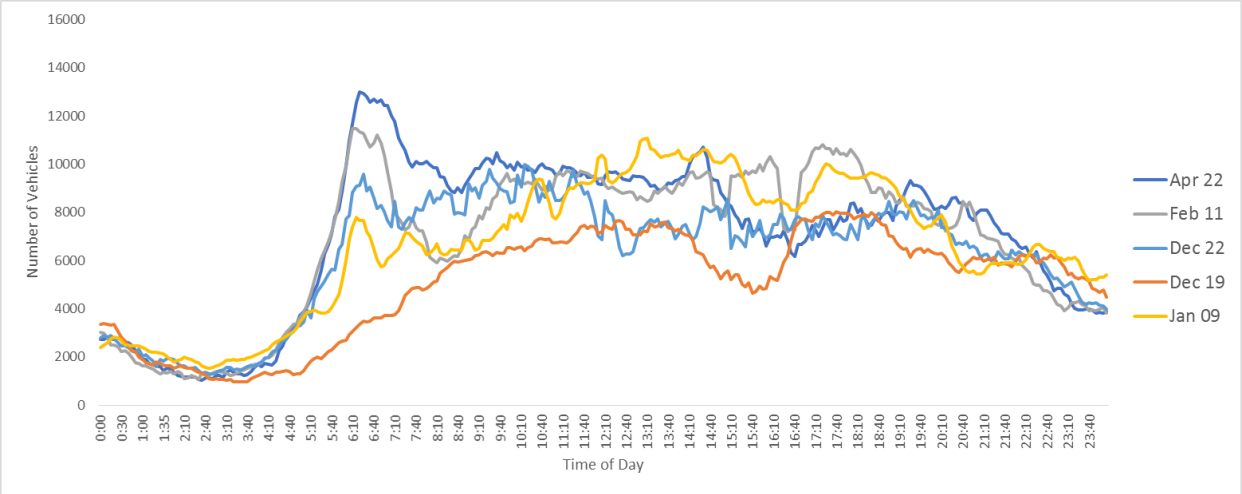

Figure 5-6: Extended Historical Demand for Selected Representative Daily Scenarios [Source: NWU]

In addition, the time-dependent link count on selected observation links within the Chicago Testbed are used with dynamic traffic assignment models for calibrating time-dependent OD matrix. The characteristics of traffic count data used in this project are shown in Table 5-3 and Figure 5-7. The unselected detectors on the freeways are excluded due to insufficient observations for the selected representative daily scenarios. Please note that the hypothetical cluster Cluster B-7 will adopt the weather and traffic demand operational conditions for Cluster B-4. The influence of incidents will be hypothetically tested on highways.

Table 5-3: Characteristics of Traffic Data Sources

Facility Type	Freeway (I-94, I-90,I-290 and Lakeshore Drive)
Data Source	Traffic Systems Center (TSC) of Illinois DOT
Resolution	5 minute
Data Contents	flow, speed, occupancy

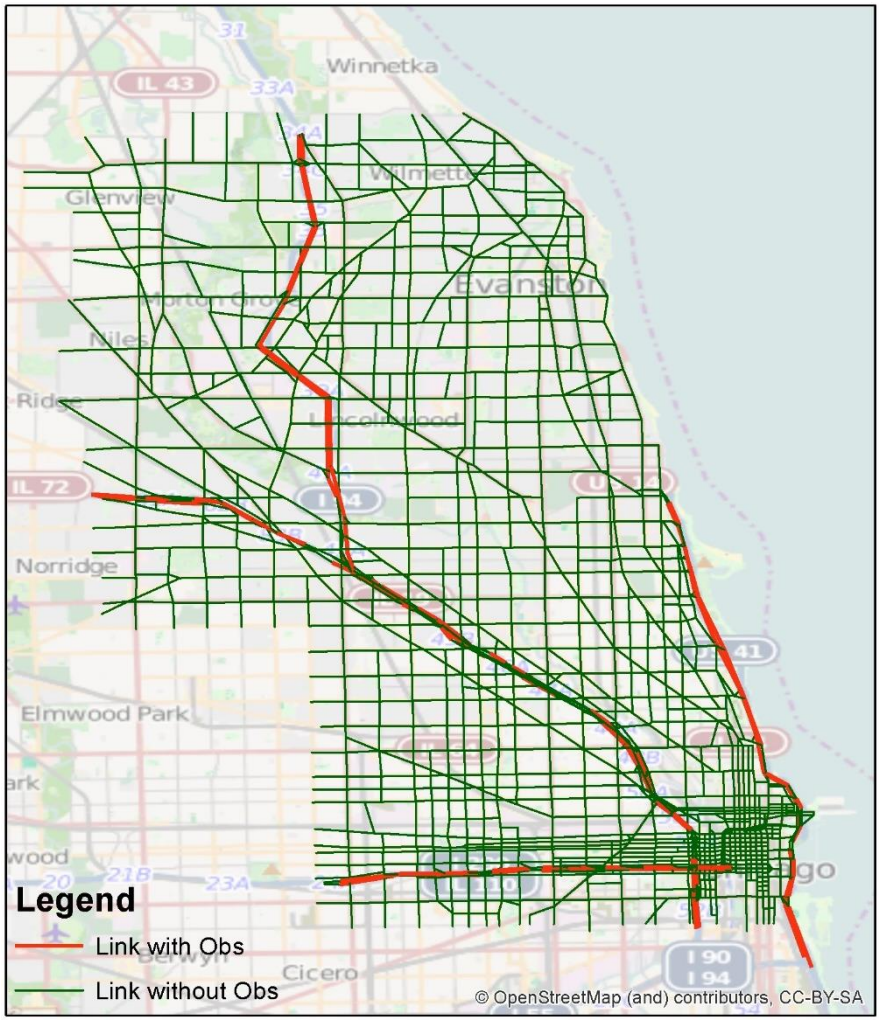

Figure 5-7: Obtained Locations of Traffic Counts Data [Source: Open Street Map]

5.4.2 Weight Parameter Settings

In each DTA simulation, 10 iterations of the User Equilibrium algorithm are applied to reach an equilibrium state in the network. Initially, a sensitivity analysis on parameter *w* for Eq. (4-14) is conducted to select optimal weights in the objective function for the deviation from historical demand and link counts. The sensitivity analysis includes two ranges of values for the parameter *w*. The first range includes 0.1 to 0.9, with increments of 0.1, for the deviation from historical demand. The second range includes the following values: 0.99, 0.999 and 0.9999. **Error! eference source not found.** shows deviations from observations and the deviation from the target demand under different weight selections in the first iteration of the basic solution method. By comparison it can be seen that *w*=0.99 gives the best compromise between two deviation terms in the objective function and is selected for numerical experiments.

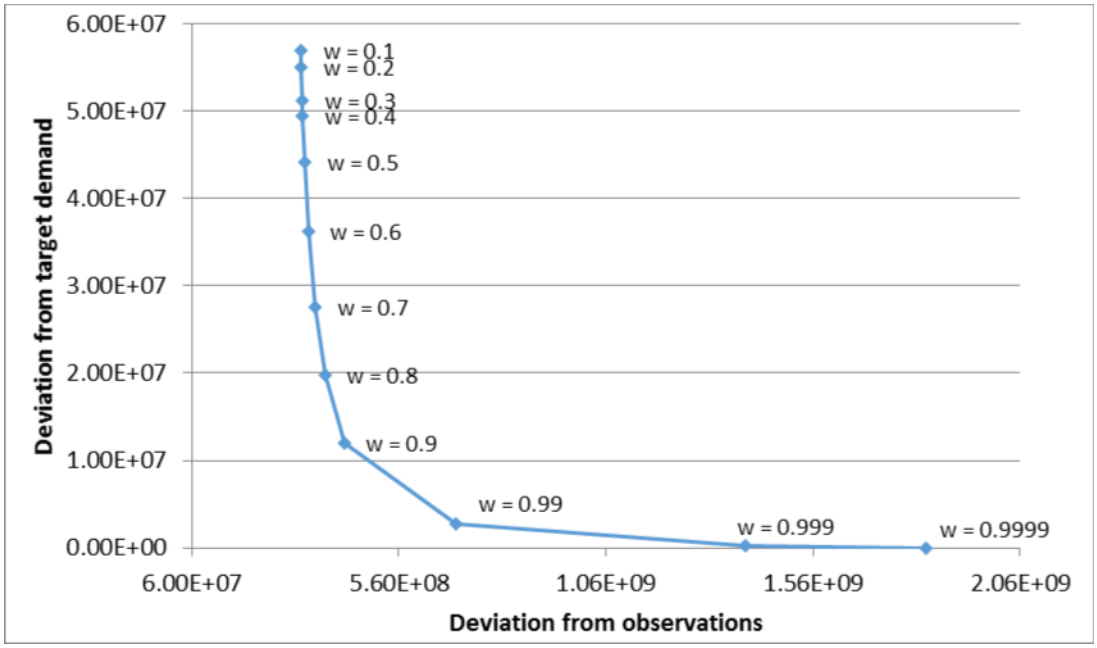

Figure 5-8: Sensitivity Analysis of Different Weights [Source: NWU]

The link weights are set to a default value of 1 for all links with observations. The time weights or the 288 intervals (total of 24 hours) of demand vary from period to period. In this study, the time weights for peak hours (6:00AM to 8:30AM and 5:00PM to 7:30PM) are set to 3, the time weights for the high demand off peak (8:30AM to 2:00PM and 7:30PM to 9:00PM) are set to 2, and the remaining intervals are set to the default value.

With the data prepared and weights set, the TDOD matrix is calibrated by the procedures described in Section 4.3. For each scenario, the overall OD demand pattern is compared before and after TDOD estimation. The following subsections present the temporal distributions of vehicles in the historical OD matrix (denoted by "Old Demand") and the most up-to-date time-dependent OD matrix (denoted by "New Demand").

5.4.3 Representative Daily Scenario Calibration

5.4.3.1 Cluster B-0: April 22

Table 5-4 shows the estimation results for the scenario on April 22. The first part represents the number of vehicles after each iteration. The second part shows the RMSE values that are discussed in the previous section (i.e., RMSEDemand and RMSEFlows). Since the target demand is generated from calibrated peak hour demand, the objective function converges after 4 iterations. The RMSEDemand is stabilizing around 0.094. Figure 5-9 presents the temporal distributions of trips for the original static OD matrix (denoted by "Old Demand") and the most up-to-date time-dependent OD matrix (denoted by "New Demand").

Table 5-4: RMSE Values for the scenario on April 22.

	Number of Trips	RMSE Values		Rate of Convergence		
		$RMSE_{Demand}$	**$RMSE_{Flows}$**	**$RMSE_{Demand}$**	**$RMSE_{Flows}$**	**Overall**
Historical OD matrix	2,041,675	0.000*	386.934	0.000*	0.000*	0.000*
New time-dependent OD matrix after **Iteration 1**	2,200,868	0.08	371.194	8.00%	4.07%	12.07%
New time-dependent OD matrix after **Iteration 2**	2,267,675	0.094	363.646	17.50%	2.03%	19.53%
New time-dependent OD matrix after **Iteration 3**	2,319,247	0.097	355.131	3.19%	2.34%	5.53%
New time-dependent OD matrix after **Iteration 4**	2,281,141	0.094	355.181	3.09%	0.01%	3.11%

** Deviation and Convergence Rate are zero because they represent the deviation between the static OD matrix and itself.*

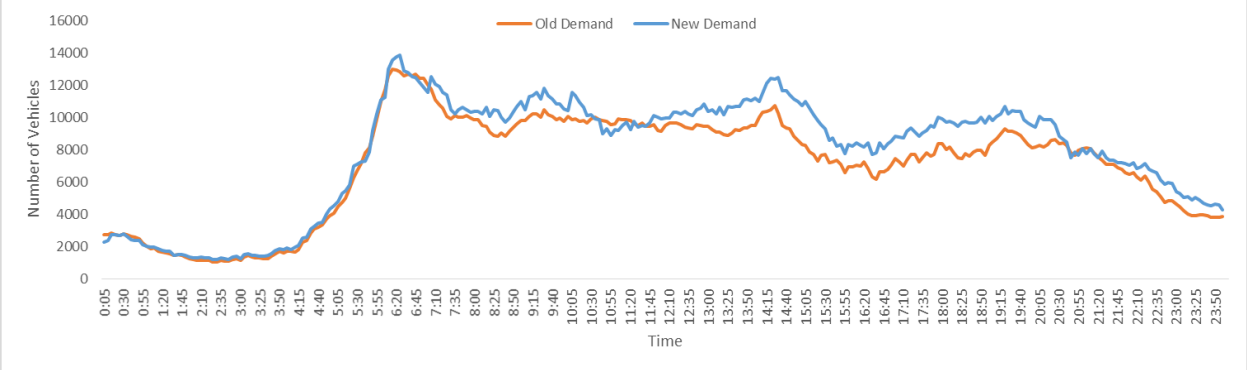

Figure 5-9: Temporal Distribution of Vehicles for the Scenario on April 22 [Source: NWU]

5.4.3.2 Cluster B-3: February 18

Table 5-5 shows the estimation results for the scenario on February 18. The first part represents the number of vehicles after each iteration. The second part shows the RMSE values that are discussed in the previous section (i.e., RMSEDemand and RMSEFlows). Since the target demand is generated from calibrated peak hour demand, the objective function converges after 5 iterations. The RMSEDemand is stabilizing around 0.062. Figure 5-10 presents the temporal distributions of trips of the original static OD matrix (denoted by “Old Demand”) and the most up-to-date time-dependent OD matrix (denoted by “New Demand”).

Table 5-5: RMSE Values for the scenario on February 18

	Number of Trips	RMSE Values		Rate of Convergence		
		$RMSE_{Demand}$	**$RMSE_{Flows}$**	**$RMSE_{Demand}$**	**$RMSE_{Flows}$**	**Overall**
Historical OD matrix	1,979,013	0.000*	321.749	0.000*	0.000*	0.000*
New time-dependent OD matrix after **Iteration 1**	2,016,750	0.092	319.352	9.20%	0.74%	9.94%
New time-dependent OD matrix after **Iteration 2**	2,035,117	0.085	314.955	7.61%	1.38%	8.99%
New time-dependent OD matrix after **Iteration 3**	1,963,443	0.059	306.031	30.59%	2.83%	33.42%
New time-dependent OD matrix after **Iteration 4**	1,980,531	0.061	305.343	3.39%	0.22%	3.61%
New time-dependent OD matrix after **Iteration 5**	1,982,151	0.062	303.995	1.64%	0.44%	2.08%

** Deviation and Convergence Rate are zero because they represent the deviation between the static OD matrix and itself*

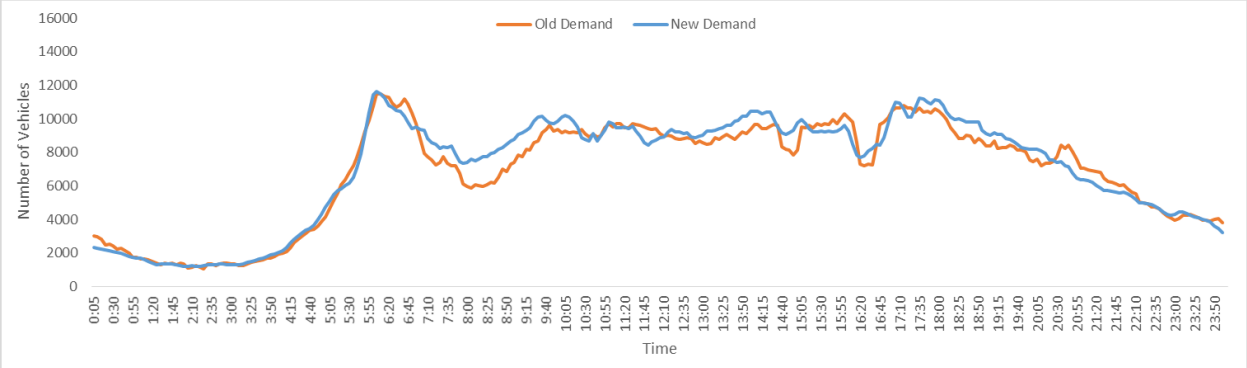

Figure 5-10: Temporal Distribution of Vehicles for the Scenario on February 18 [Source: NWU]

5.4.3.3 Cluster B-4: December 22

Table 5-6 shows the estimation results for the scenario on December 22. The first part represents the number of vehicles after each iteration. The second part shows the RMSE values that are discussed in the previous section (i.e., RMSEDemand and RMSEFlows). Since the target demand is generated from calibrated peak hour demand, the objective function converges after 3 iterations. The RMSEDemand is stabilizing around 0.033. Figure 5-11 presents the temporal distributions of trips of the original static OD

matrix (denoted by “Old Demand”) and the most up-to-date time-dependent OD matrix (denoted by “New Demand”).

Table 5-6: RMSE Values for the scenario on December 22

	Number of Trips	RMSE Values		Rate of Convergence		
		$RMSE_{Demand}$	**$RMSE_{Flows}$**	**$RMSE_{Demand}$**	**$RMSE_{Flows}$**	**Overall**
Historical OD matrix	1,830,809	0.000*	333.471	0.000*	0.000*	0.000*
New time-dependent OD matrix after **Iteration 1**	1,810,242	0.061	315.829	6.10%	5.29%	11.39%
New time-dependent OD matrix after **Iteration 2**	2,060,893	0.032	310.070	47.54%	1.82%	49.36%
New time-dependent OD matrix after **Iteration 3**	2,061,936	0.033	304.734	3.13%	1.72%	4.85%

** Deviation and Convergence Rate are zero because they represent the deviation between the static OD matrix and itself.*

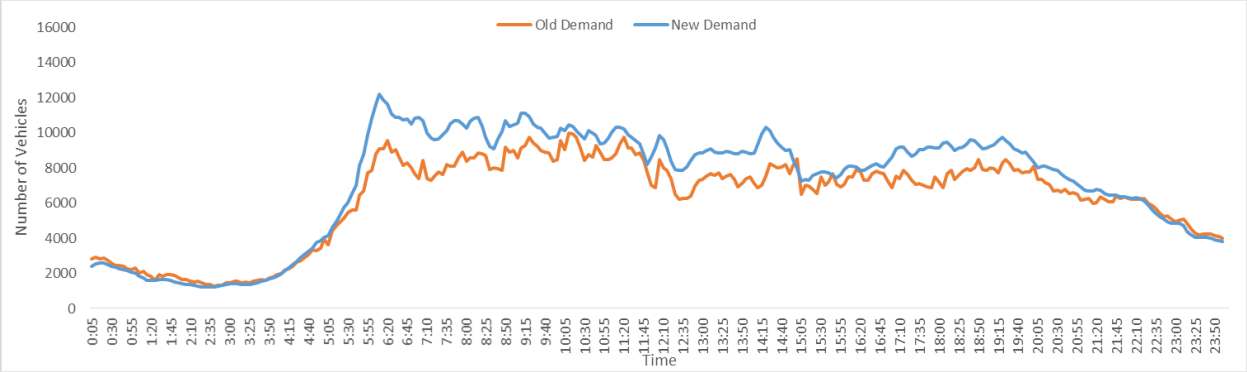

Figure 5-11: Temporal Distribution of Vehicles for the Scenario on December 22 [Source: NWU]

5.4.3.4 Cluster C-4: December 19

Table 5-7 shows the estimation results for the scenario on December 19. The first part represents the number of vehicles after each iteration. The second part shows the RMSE values that are discussed in the previous section (i.e., RMSEDemand and RMSEFlows). Since the target demand is generated from calibrated peak hour demand, the objective function converges after 4 iterations. The RMSEDemand is stabilizing around 0.023. Figure 5-12 presents the temporal distributions of trips of the original static OD matrix (denoted by “Old Demand”) and the most up-to-date time-dependent OD matrix (denoted by “New Demand”).

Table 5-7: RMSE Values for the scenario on December 19

	Number of Trips	RMSE Values		Rate of Convergence		
		$RMSE_{Demand}$	**$RMSE_{Flows}$**	**$RMSE_{Demand}$**	**$RMSE_{Flows}$**	**Overall**
Historical OD matrix	1,465,204	0.000*	307.454	0.000*	0.000*	0.000*
New time-dependent OD matrix after **Iteration 1**	1,820,665	0.031	292.283	3.10%	4.93%	8.03%
New time-dependent OD matrix after **Iteration 2**	1,725,752	0.026	289.168	16.13%	1.07%	17.19%
New time-dependent OD matrix after **Iteration 3**	1,655,296	0.022	279.187	15.38%	3.45%	18.84%
New time-dependent OD matrix after **Iteration 4**	1,695,502	0.023	275.683	3.55%	1.26%	4.81%

* Deviation and Convergence Rate are zero because they represent the deviation between the static OD matrix and itself.'

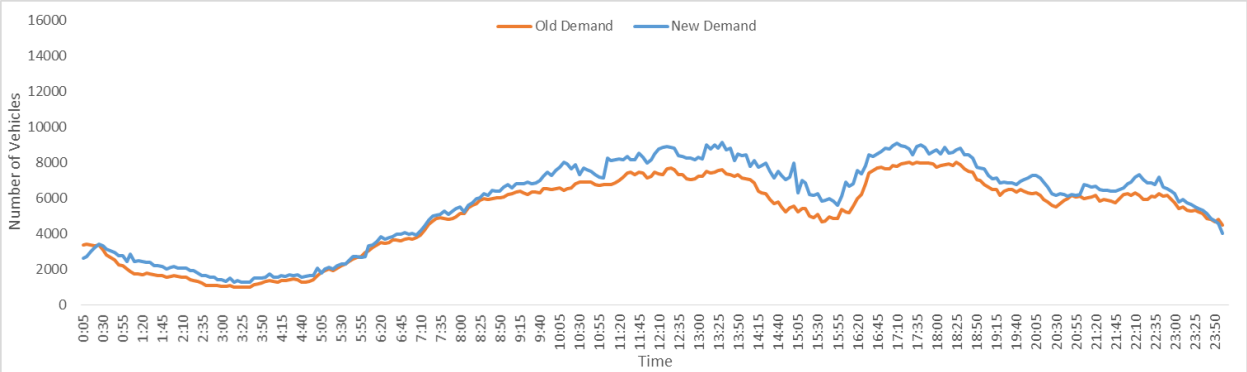

Figure 5-12: Temporal Distribution of Vehicles for the Scenario on December 19 [Source: NWU]

5.4.3.5 Cluster B-6: January 09

Table 5-8 shows the estimation results for the scenario on January 09. The first part represents the number of vehicles after each iteration. The second part shows the RMSE values that are discussed in the previous section (i.e., RMSEDemand and RMSEFlows). Since the target demand is generated from calibrated peak hour demand, the objective function converges after 4 iterations. The RMSEDemand is stabilizing around 0.040. Figure 5-13 presents the temporal distributions of trips of the original static OD matrix (denoted by "Old Demand") and the most up-to-date time-dependent OD matrix (denoted by "New Demand").

Table 5-8: RMSE Values for the scenario on January 09

	Number of Trips	RMSE Values		Rate of Convergence		
		$RMSE_{Demand}$	**$RMSE_{Flows}$**	**$RMSE_{Demand}$**	**$RMSE_{Flows}$**	**Overall**
Historical OD matrix	1,914,517	0.000*	324.427	0.000*	0.000*	0.000*
New time-dependent OD matrix after **Iteration 1**	1,823,805	0.084	273.035	8.40%	15.84%	24.24%
New time-dependent OD matrix after **Iteration 2**	1,746,351	0.05	266.212	40.48%	2.50%	42.98%
New time-dependent OD matrix after **Iteration 3**	1,754,568	0.042	258.926	16.00%	2.74%	18.74%
New time-dependent OD matrix after **Iteration 4**	1,752,470	0.041	253.483	2.38%	2.10%	4.48%

* Deviation and Convergence Rate are zero because they represent the deviation between the static OD matrix and itself.

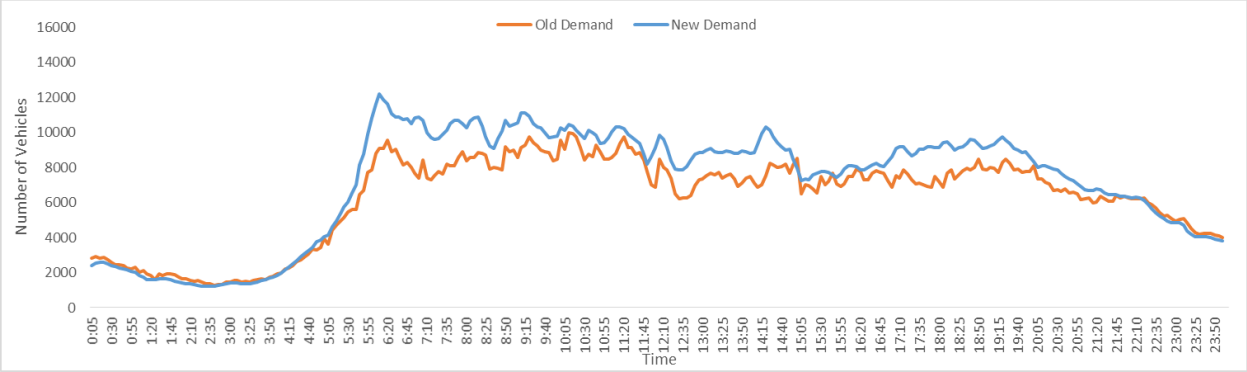

Figure 5-13: Temporal Distribution of Vehicles for the Scenario on January 09 [Source: NWU]

5.5 Calibration Results Verification

In this section, the TDOD estimation is first validated by a link-level validation, and then the overall calibration results, including the traffic flow model, WAF and TDOD are taken into DYNASMART-X and verified by the comparison between simulation data and historical observation data.

First, the simulated and observed link counts are compared for several selected links. Simulated results based on the estimated time-dependent OD matrix are compared with the actual observations, which are collected during the time period that corresponds to the demand horizon

used for the OD matrix estimation.

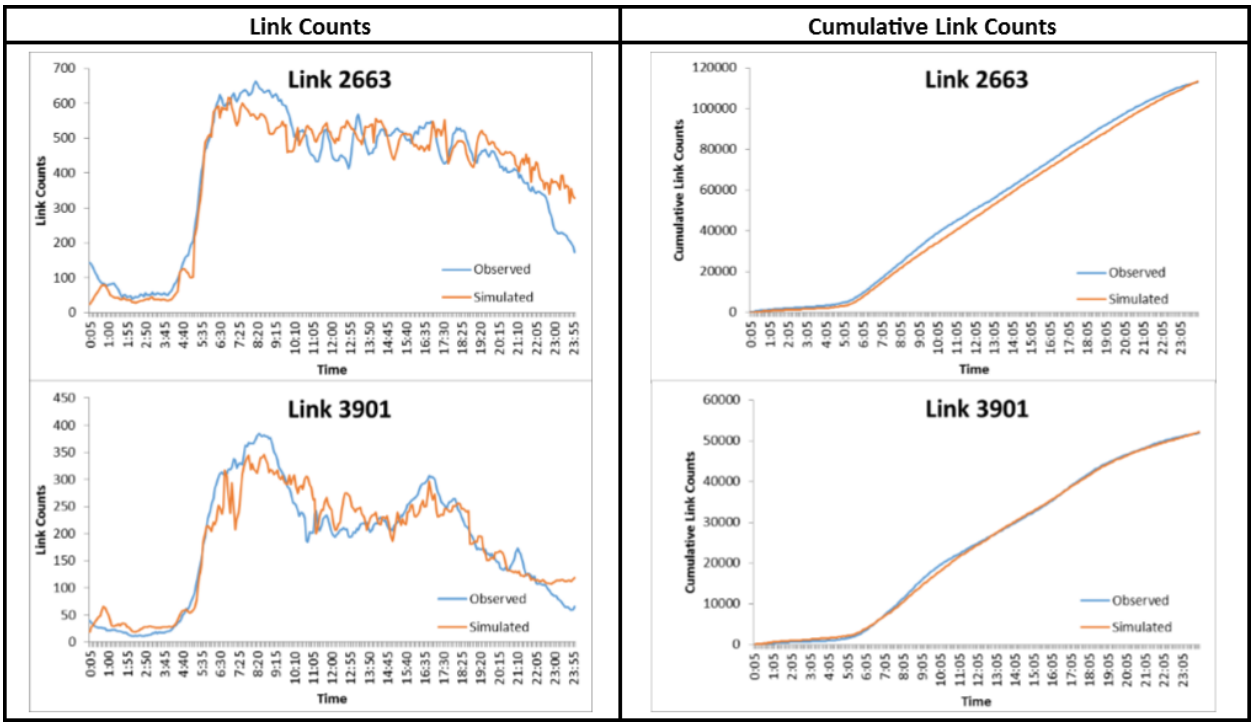

Figure 5-14 to

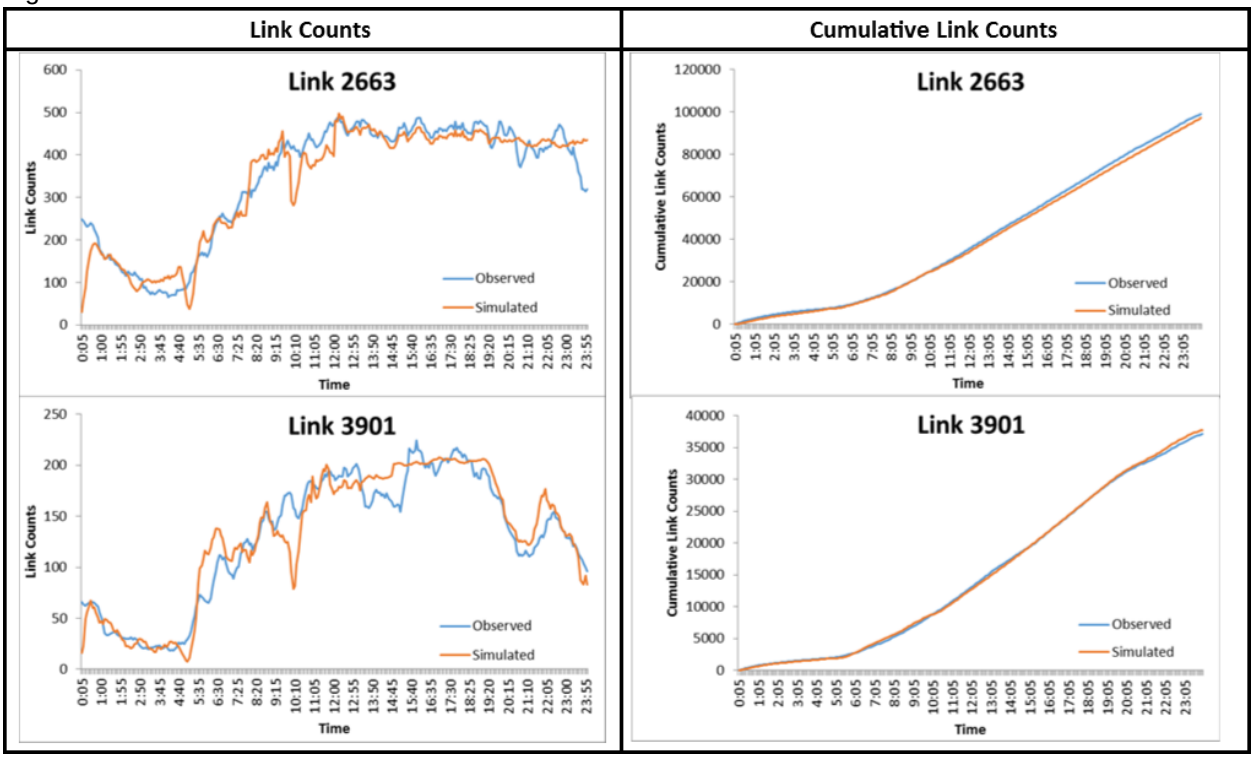

Figure 5-18 display the number of vehicle counts (left column) and the 5-minute cumulative vehicle counts (right column) for two selected links, respectively. Overall, link-level comparisons show good agreement.

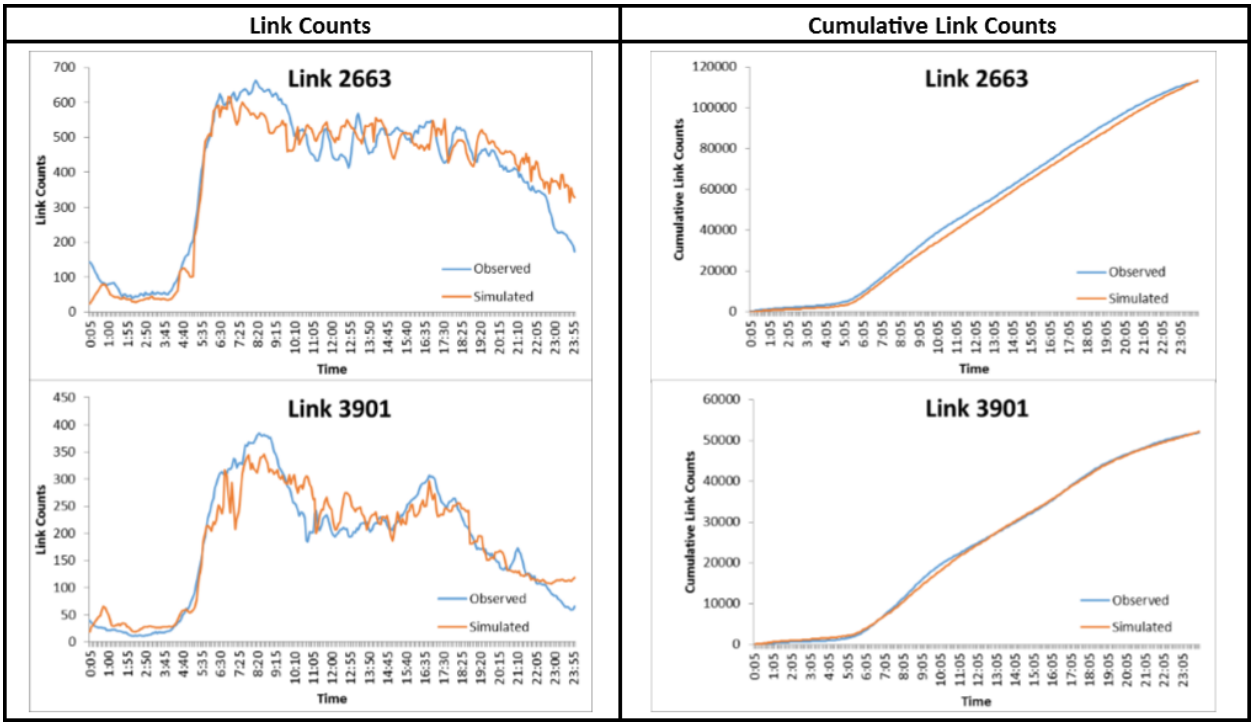

Figure 5-14: Observed and Simulated Counts on Selected Links for the Scenario on April 22 [Source: NWU]

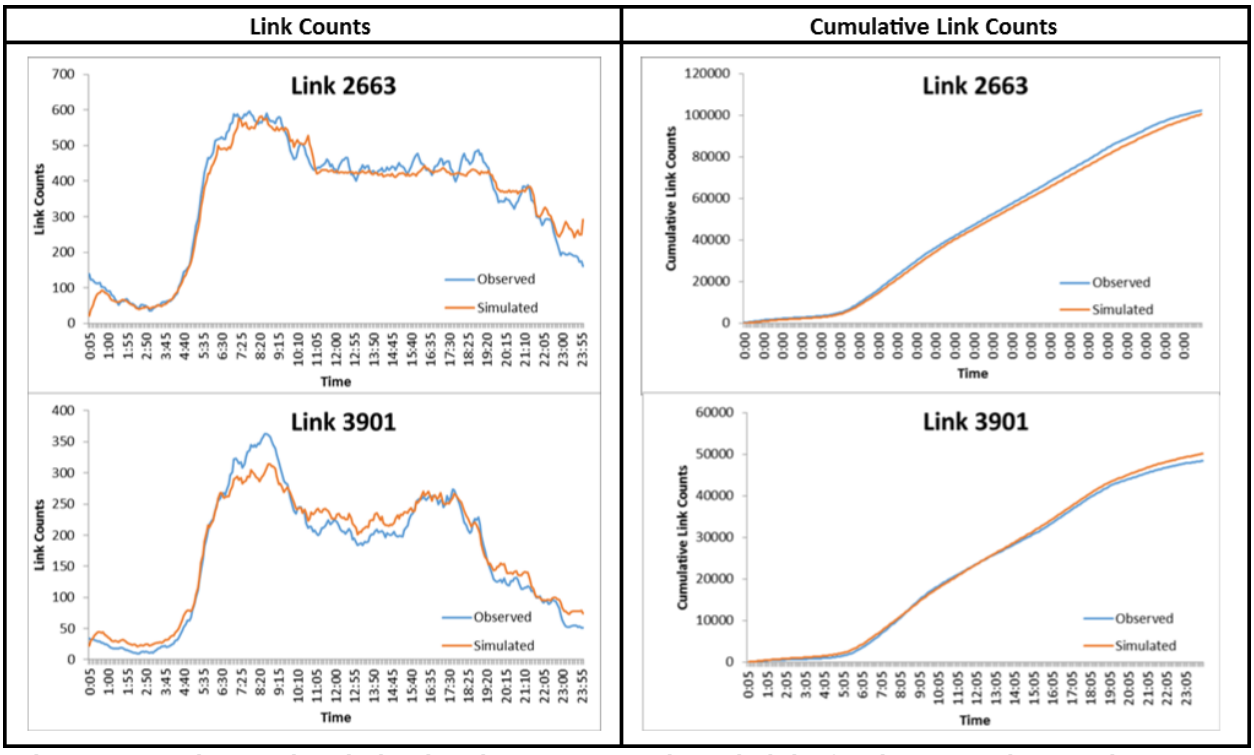

Figure 5-15: Observed and Simulated Counts on Selected Links for the Scenario on February 18. [Source: NWU]

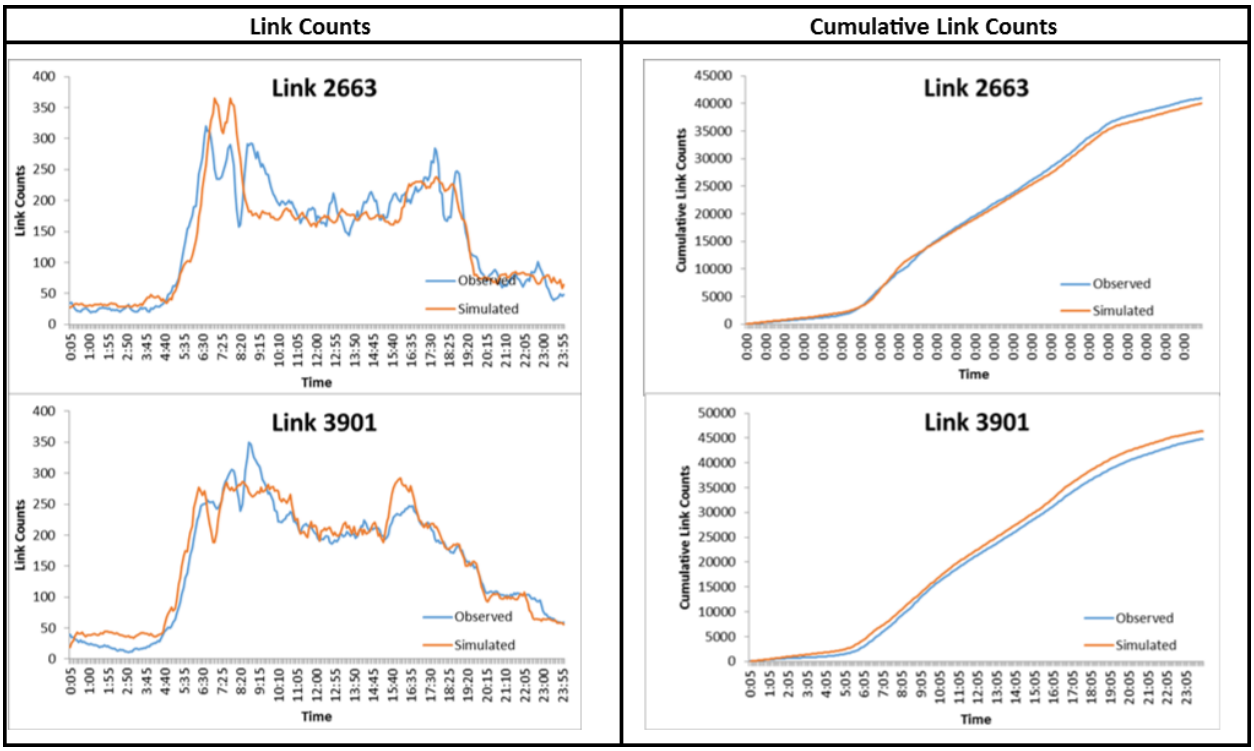

Figure 5-16: Observed and Simulated Counts on Selected Links for the Scenario on December 22 [Source: NWU]

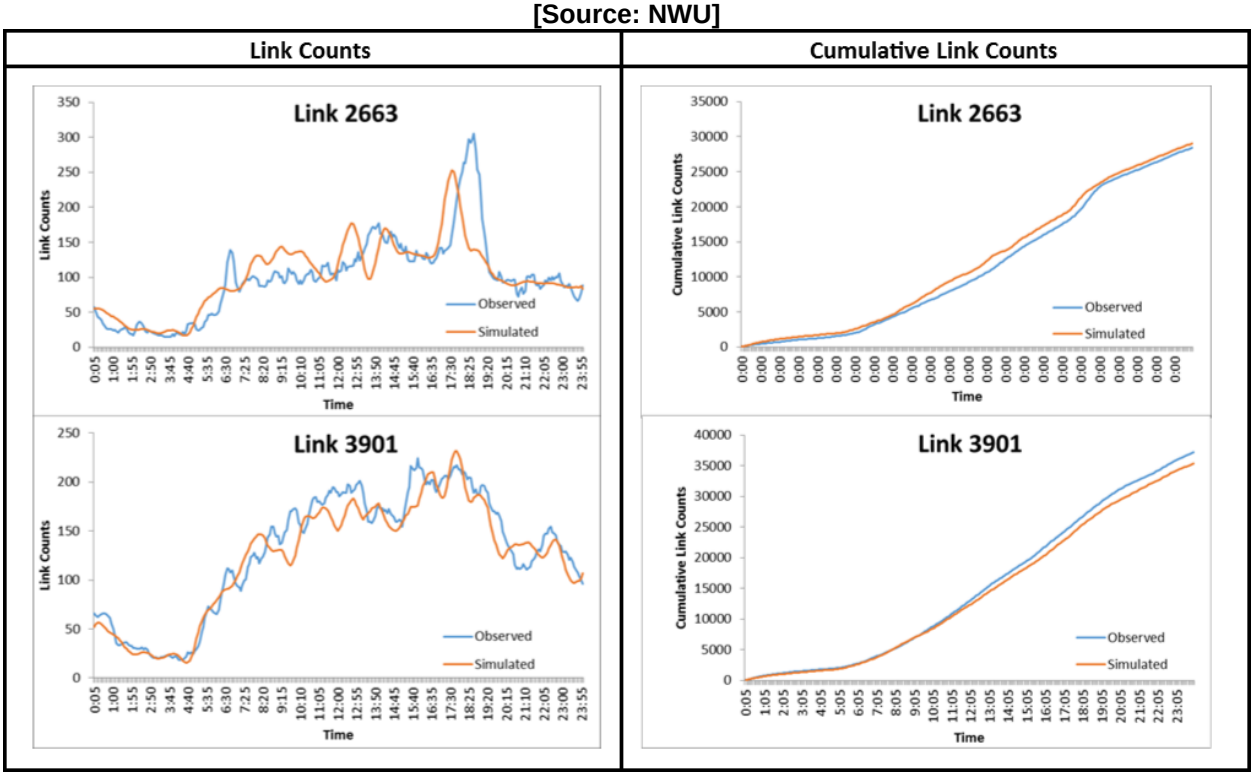

Figure 5-17: Observed and Simulated Counts on Selected Links for the Scenario on December 19 [Source: NWU]

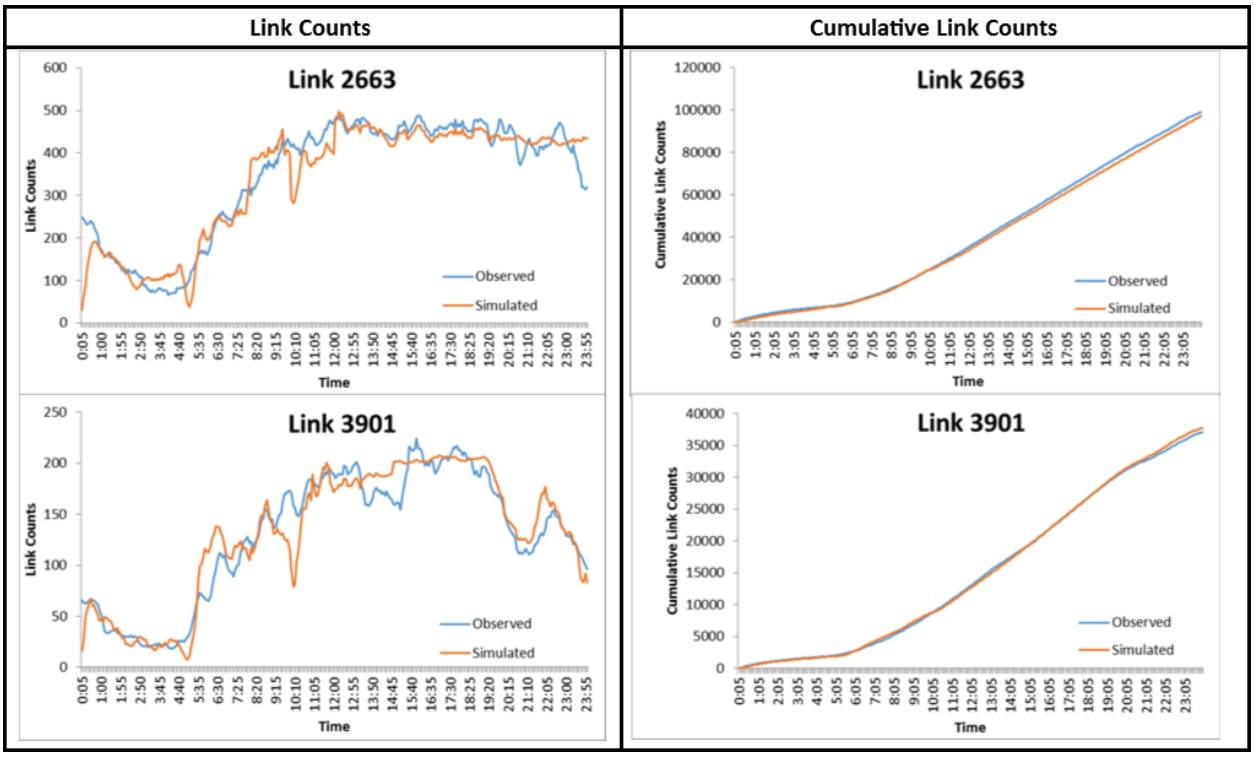

Figure 5-18: Observed and Simulated Counts on Selected Links for the Scenario on January 09 [Source: NWU]

OD estimation based on cluster results and network parameter calibration are tested and verified with the simulation tool, DYNASMART, by comparing its system performance indicator, in this case speed, with the historical observed speed. The two selected links are located in the Eastbound of I90 Kennedy Expressway (Link 4800) and the Northbound of North Lake Shore Drive (Link 3656). Since DYNASMART produces estimated system performance every 60 seconds, while the time resolution for historical data is 5 minutes, the link speed verification is aggregated to 15-minute intervals for 24 hours for each representative daily scenario.

Figure 5-19 depicts the verification results for the five clusters, where the blue line with diamond marks represents the estimation results, the grey line with round marks illustrates the historical speed observation obtained from loop detectors, and the green band represents the acceptance threshold. It is worth noting that the width of the threshold varies every interval. For each cluster, the threshold is calculated as the standard deviation within every interval according to all daily scenarios in that cluster. The upper bound of the threshold band is the observed speed plus the standard deviation at current interval calculated from the observations, while the lower bound is the observed speed minus the standard deviation. If the estimated speed is larger than the upper bound, we consider these results as “over-estimated”; if it is smaller than the lower bound, the speed is considered under-estimated. Visual inspection reveals overall good fit within the considered bands.

Table 5-9 summarizes the link speed verification results. The threshold to pass the verification is that the acceptance ratio is no less than 80% for the adverse weather affected scenarios and 85% for the other scenarios. The best case is December 19 for Cluster C-4.Cluster C-4 is a weekend cluster, where the overall demand is lower than other clusters, and the speed distribution in Figure 5-19 (e-f) is more stable than other clusters. Link 4800 in December 22 for Cluster B-4 also did not exhibit particularly good fit—however, the over estimation occurs during the middle of the night, where the simulated free flow speed is

somewhat higher than the observation during the system warming up process; furthermore, the simulated recovery process after the afternoon peak hour appears to be a little slower than the observation. The worst case is January 09 for Cluster B-6. Cluster B-6 is a weekday cluster with heavy snow, where link 4800 almost went into breakdown with speed less than 10 mph, and link 3656 also exhibits a speed reduction in the morning peak, which did not occur for any other cluster.

Overall, instances of over- or under- estimation are limited, and apply to only relatively short periods of the day. Keeping in mind that we are comparing the estimated results from a large number of days to a single-day instance for a given cluster, which is itself a realization from a stochastic process with high variability, these results suggest that the model is well capable of capturing the intended system performance for the intended purpose of the evaluation.

Table 5-9: The Link Speed Verification Summary

		Over Estimation	Under Estimation	Acceptance Ratio
B-0: Apr 22	L4800	10.42%	1.04%	88.54%
	L3656	0.00%	3.13%	96.88%
B-3: Feb 18	L4800	6.25%	6.25%	87.50%
	L3656	0.00%	7.29%	92.71%
B-4: Dec 22	L4800	7.29%	9.38%	83.33%
	L3656	0.00%	7.29%	92.71%
C-4: Dec 19	L4800	1.04%	0.00%	98.96%
	L3656	0.00%	6.25%	93.75%
B-6: Jan 09	L4800	10.42%	9.38%	80.21%
	L3656	9.38%	2.08%	88.54%

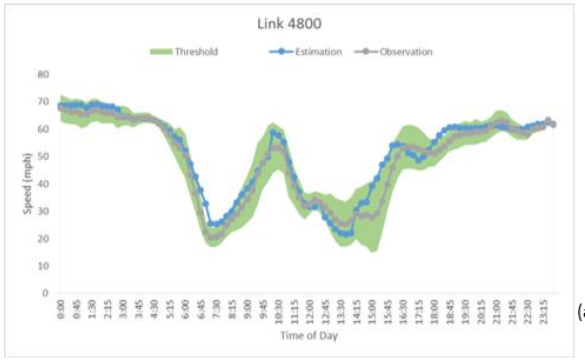

(a)

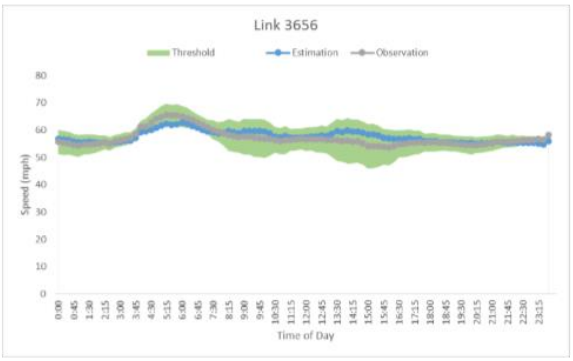

(b)

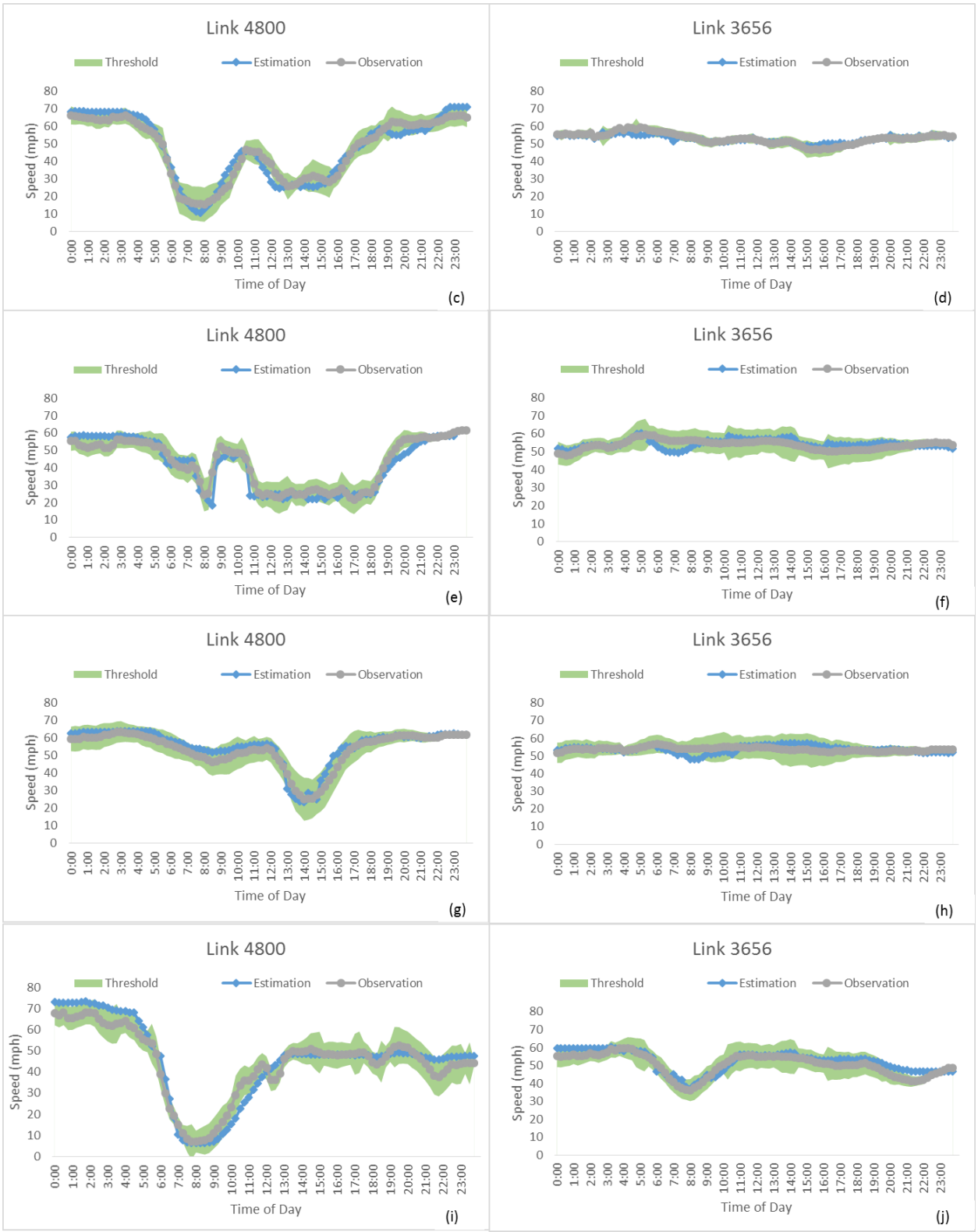

Figure 5-19: The speed verification on selected links: (a-b) April 22; (c-d) February 18; (e-f) December 22; (g-h) December 19; (i-j) January 09 [Source: NWU]

Chapter 6. Summary

This report presents the methodology used to calibrate the DYNASMART model for the representative daily scenarios for selected clusters that were identified to examine the effectiveness of the different ATDM and DMA strategies in the Chicago Testbed. The calibration methodology involves adjusting the parameters of the traffic flow model for the different highway links, the weather adjustment factor (WAF), and the time-dependent OD demand matrix for these representative daily scenarios. Based on the calibration effort conducted in this study, a set of results that illustrate the estimated and observed time-varying link flows as well as the speed profiles are presented.

It is worth mentioning that the calibration of such large-scale simulation models is a challenging task. First, not all of the network links have installed sensors in the existing traffic system. In the Chicago Testbed, loop detector data are only reliably available for freeway and major highway links. These were used here and in previous studies. Nonetheless, the calibration process has produced satisfactory results in terms of the three main criteria used: (1) minimizing the deviation between estimated TDOD values and all available time-varying volume observations, (2) minimizing the deviation between the estimated TDOD values and the static target matrix adopted by the planning agency; and (3) replicating cumulative time-varying flow patterns on individual links. The validation results confirm that the model is capable of reproducing the observed flow patterns for each of the cluster day representatives.

It should be noted that the joint estimation of the entire 24-hr TDOD demand pattern, for each cluster, is a novel application introduced in this study. Most previous DTA applications are limited to peak-period demands. When 24-hr runs are conducted, it will construct the 24-hr demand by extrapolating estimated OD demand from the peak period to an overall daily pattern. The approach used here is possible because of powerful estimation tools such as the KNiTRO non-linear optimization software, as well as improvements in representation applied to reduce the problem dimensionality. We believe that the ability to conduct 24-hr analyses is particularly valuable and appropriate to evaluate weather-related ATDM and DMA interventions, which will typically have a substantial effect outside of the normal (good weather) peak periods.

Completing the calibration of the baseline and other selected scenarios is a significant milestone for this project. The next steps involve finalizing the experimental design and perform the simulation experiments to answer the research questions defined as part of this project.

U.S. Department of Transportation
ITS Joint Program Office-HOIT
1200 New Jersey Avenue, SE
Washington, DC 20590

Toll-Free “Help Line” 866-367-7487
www.its.dot.gov

FHWA-JPO-16-381

U.S. Department of Transportation